WYLE LABORATORIES
TESTING DIVISION, HUNTSVILLE FACILITY

research p

WYLE LABORATORIES - RESEARCH STAFF

TECHNICAL REPORT WR 68-4

AN INVESTIGATION TO LOCATE THE ACOUSTIC SOURCES IN A HIGH SPEED JET EXHAUST STREAM

by

R. C. Potter

Submitted Under Contract NAS8-21060

Date February 1968

Copy No. 5

El Segundo Facility
El Segundo, California 90245

SUMMARY

A small high speed (Mach 2.5) cold jet was operated with the exhaust stream passing through a hole in the wall of a 100,000 cubic foot reverberation room. The reverberant SPL was measured to allow determination of the total acoustic power generated by the flow inside the room. The jet nozzle was then progressively withdrawn, so that a smaller amount of the mixing flow was retained within the room. The experiment was repeated with the jet inside the room, with the flow directed outwards, and the jet nozzle moved back into the room. The resultant acoustic power curves were differentiated to give the acoustic power generated per unit length of the jet flow. The results for the total acoustic power and octave band power distributions are presented and experimental details reviewed. It is concluded that the flow near the supersonic core tip is responsible for the majority of the noise generated.

TABLE OF CONTENTS

1.0 INTRODUCTION

The accurate definition of the acoustic source distribution in a jet stream will allow a positive analysis for jet noise control by nozzle and suppressor design. The way a jet flow mixes with the atmosphere to create sound is complicated, especially for high speed jets where the mechanism can involve several different kinds of processes. Theoretical and experimental studies of jet noise in the past have been in terms of generalized results and an accurate definition of source properties has not been forthcoming.

Experimental measurements of the near and far sound field of jets have indicated a basic difference between sound generated by subsonic and high speed supersonic rocket exhaust. These observations have indicated that the major source region for a subsonic jet is the initial mixing flow near the nozzle, while the region of maximum noise production for a supersonic jet flow appears to occur at a point downstream from the nozzle.

Theoretical evaluation has further confused the understanding of this problem. Ribner (Reference 1) and Lilley (Reference 2), following Lighthill's analysis of aerodynamic noise generation (References 3 and 4) have shown the initial mixing region of a subsonic jet to be the main acoustic source region. By use of the normalized results for assumed flow similarity regions, they determined the well known x^0 and x^{-7} power laws for the acoustic source strength in the initial mixing region and the far downstream fully developed turbulent flow region respectively. This was in agreement with the generally observed experimental results.

However, the analysis of supersonic turbulent flows by Ffowcs-Williams (Reference 5) suggested that the initial flow near the nozzle was also the major source region for high speed supersonic jet flows. This was in disagreement with the experimental evidence (References 6 and 7). The near field acoustic measurements have been criticized on two accounts. First a microphone in the near field will not measure

acoustic intensity exactly because of the difference in phase between particle velocity and pressure in this hydrodynamic region. Secondly, a microphone will respond to sound radiated from points other than directly opposite it in the flow.

It was with this disagreement in mind, that the experiments reported here were designed. The objective was to develop an experimental technique to obtain accurate measurements of the acoustic source distribution in jet flows, and then to examine the source distribution in various classes of jet flows. The technique developed involved firing a small jet through an orifice into a large reverberation room and separating the jet flow into two parts; one part within the room for which the total acoustic power generated can be measured, and one part outside the room whose sound field is excluded. The acoustic source distribution could then be determined absolutely by positioning the jet to include various portions of the jet flow within the room.

Results are presented for a Mach 2.5, 1860 fps nitrogen jet, which was the first of a series of hot and cold subsonic, supersonic and rocket exhaust flows to be examined. The following sections give a brief description of the apparatus used in the experiment, the results obtained, the examination of orifice size, shape and edge effects on the noise field generated, and the analysis used to obtain the source distribution results. A final section summarizes the conclusions of this report and indicates the importance of the downstream portion of the flow to the total sound generated by this particular jet.

2.0 DESCRIPTION OF THE APPARATUS AND EXPERIMENTAL TECHNIQUE

Figure 1 illustrates the technique used to obtain the measurements reported here. The sketch shows a small jet fired through a hole in the wall of a large reverberation room. The total sound power generated in the room is then determined by measuring the reverberant sound pressure level and correcting for the absorption characteristics of the room. By positioning the jet at different distances from the orifice, a varying amount of the mixing flow was contained within the room.

The jet flow used was that from a nitrogen storage tank to give a fully expanded Mach 2.5 jet with an exit diameter of one inch. The room used had an internal volume of 100,000 cubic feet, which was more than sufficient to insure that the sound field in the room would not affect the acoustic source characteristics, Figures 2 and 3. The perfectly expanded computer designed nozzle gave a jet exit Mach number of 2.49, with a jet exit velocity of 1860 fps, when operated at the correct pressure ratio. The flow was examined using a shadowgraph technique and was observed to be fully expanded with no noticeable shock wave structure. Nitrogen gas was chosen for the flow because of its availability and convenience for accurate control.

A plenum was used to settle the gas before the nozzle; Figure 4 shows a photograph of the plenum and nozzle set up in front of an orifice plate.

Microphones were positioned both inside and outside of the room, with the inside microphones located at several points, some near the source, to insure the most accurate reverberant sound pressure level was determined. Data was initially acquired on tape, but all later measurements involved on-line analog data reduction to insure that the highest frequencies were covered. The jet was first operated with the flow directed through the orifice and into the reverberation room, with the nozzle being progressively moved away from the wall. Then the nozzle was set up inside the room, with the jet being directed through the orifice

and out of the room. The nozzle was next moved back within the chamber so that the larger amount of flow was contained within the room.

All orifices were constructed in 3/4 - inch thick aluminum plates and were positioned in the center of one of the walls of this reverberation room. For each nozzle-to-orifice separation, different orifice sizes were examined and, once a size to give minimum disturbance to the flow field and to the resultant sound pressure level inside the room was determined, a standard ratio of nozzle exit diameter to jet flow diameter was held for all separation distances. The shadowgraph photographs of the jet flow were used to judge the size of orifice required. Additionally, the effects of the orifice edge shape were further examined. Certain hole tones were created, and this extraneous effect was examined and eliminated from the results reported here. The details of these effects will be discussed in later sections of the report.

Table I is a list of the runs completed in these experiments and indicates all relevant parameters and dimensions.

3.0 DATA REDUCTION

In order to convert the reverberant sound pressure levels measured in the room to acoustic power, the reverberation characteristics of the room are required. Figure 5 shows the measured reverberation time for the chamber (time for the level to fall 60 dB) and the corresponding absorption of the room in Sabins (ft^2). The figure also shows the calculated high frequency absorption for various humidities, where the absorption is controlled by the molecular atmospheric absorption in the room. The results show a constant low frequency absorption of just over 200 equivalent ft^2 up to a frequency of 500 Hz. Above this frequency, the atmospheric absorption becomes the controlling factor. The results show the importance of humidity, especially at the high frequencies, and it was therefore important to measure the exact conditions in the room during each test run. The jet itself consisted of dry nitrogen, however in view of the large volume of the room and the relatively small amount of gas introduced during each run, the conditions in the room were not considered to change during each run.

The acoustic power can be obtained from the reverberant sound pressure level by:

$$PWL_f = SPL_f + 10 \log_{10} a_f - 6.4 + H_f \qquad (1)$$

where PWL is the acoustic power level in dB, re: 10^{-13} watts

SPL is the reverberant sound pressure level in dB, re: 0.0002 dyne/cm^2

a is the total absorption in Sabins

and H is the correction for humidity

The subscript f indicates that the calculation must be completed at each frequency in the spectrum of the sound, and the appropriate values of absorption area and humidity correction included.

Because of the large reverberation time of the chamber (approximately 18 seconds), the sound field in the room was allowed to build up to its reverberant level before the data was recorded. After acquisition of the data, the measured sound pressure was examined for discrete frequencies by use of narrow band filters, and none were found. This was expected since the nozzle was operated at perfect expansion and no shock waves were associated with the flow. The data repeatability was checked by performing duplicate tests for many specific nozzle-to-orifice separation distances, and the results repeated remarkably well (within one dB). In addition, the levels recorded by the several microphones in the reverberant acoustic field also agreed, for a given test condition, within one dB.

The data was reduced in 1/3-octave band sound pressure level form and then, with the aid of the above relationship and the known room absorption characteristics, converted to 1/3-octave band acoustic power levels. These values were then combined to give the overall acoustic power levels.

4.0 RESULTS

Figure 6 shows a typical result for the measured reverberant sound pressure level within the room. The measured spectrum shows a rapid falloff on the high frequency power which is the result of the room characteristics. Figure 6 also shows the room correction, which is added to the results to give the total acoustic power spectrum in 1/3-octave band. These acoustic power results are then summed to give the overall acoustic power produced by that part of the jet within the room.

Figure 7 shows the spectra of acoustic power level measured for the various cases when the jet was directed into the room. This figure shows two points. Firstly, the overall sound power is reduced as the jet is removed from the wall leaving a smaller part of the flow within the room. Secondly, for the same variation, the low frequency power is increased . This increase is judged to be due to an orifice effect and will be discussed in more detail later. The general reduction in acoustic power is seen to be at the higher frequencies although no significant reduction apparently occurs until the separation distance has increased to over 13 inches (13 nozzle exit diameters). The results for the case when x = 0 inches gives the reverberant sound pressure level measured within the room for the total acoustic power of the jets, since the whole of the jet mixing flow was contained within the room in this case. Figure 8 shows this measured sound pressure level corrected with the room reverberant characteristics to give the acoustic power spectrum, directly compared to a predicted spectrum of acoustic power, derived from the results given in Reference 8. The overall acoustic power was calculated, on the basis of the acoustic power curve given in Figure 22 of Reference 8 for the 1860 fps jet of exit diameter 1 inch. to be 155.7 dB re: 10^{-13} watts. The measured total acoustic power was 152.5 dB. The spectrum was calculated on the basis of a normalized spectrum curve based on exit diameter and velocity alone and the normalized curve used is that given in Reference 8 based on the results of Reference 9. Further, to allow the spectrum shape to be better examined, the predicted overall level was adjusted to be the 152.5 dB level that was measured.

The agreement is regarded as good.

Figure 9 shows the measured spectra of acoustic power for the case when the jet was fired out of the reverberation room. In this case, the results were acquired on magnetic tape and are clipped at the higher frequencies because of the tape recorder limitations. However, they do again show the increase in power as the jet is brought back into the room and an apparent orifice effect at the lower frequencies as observed in the previously discussed results.

The total acoustic power generated for each condition is plotted in Figure 10 against distance from the nozzle to the orifice. The acoustic power is seen to remain constant as the jet is withdrawn from the room, when it is directed into the room, until the jet has been moved a distance of approximately 14 diameters out. The level then decreases rapidly for greater separations. For the case when the jet was directed out of the room, the level is seen to be small initially and increasing rapidly and then leveling off as the jet is brought back into the room. These two curves were then differentiated to obtain the acoustic source distribution in the flow.

Figure 11 shows the overall acoustic power generated per unit length, normalized on exit diameter of the nozzle, and shows a concentration of power at some 20 exit diameters from the nozzle. The two curves are for the results of the two configurations; the jet into the room and the jet directed out of the room. These results show very good agreement, and suggest that the energy loss through the orifice is very small. Because of the nature of the differentiation, the results for the jet out of the room will be more accurate for the small values of separation distance and the results for the jet into the room will be more accurate for the larger values of separation distance. This is because it is easier to determine small changes of power at lower acoustic intensities, especially where the values are read to the same accuracy on a decibel scale.

In producing these results, the values for the acoustic power at different nozzle-to-orifice distances were fitted by smoothed curves that were differentiated to give the results of Figure 11.

The initial mixing region is shown to be a very low producer of noise, and the constant x^0, as predicted for subsonic jets, is not obtained for this jet flow. Figure 12 shows the mean of these two results plotted on a log-log plot to allow the acoustic power laws to be determined. The slope of the initial acoustic power distribution curve is most effectively fitted by an x^1 curve and the downstream curve is best fitted by an $x^{-6.5}$ law. Also shown on Figures 11 and 12 are the estimated locations of the laminar core tip and the supersonic tip. The latter point is indicated as the region of most intense noise generation.

The results for 1/3-octave band acoustic power levels were combined into octave band values, and the process of plotting and differentiation repeated for 5 octave bands. The distribution of octave band acoustic power sources determined is shown in Figure 13, where the mean result of the two basic experiments are plotted and compared to the result for overall values previously determined. These results show the increasing downstream distance for the lower frequency sources. This is as expected since the turbulence properties likewise will change to larger scales and lower frequencies with downstream distance.

Figure 14 shows the normalized source spectrum at four points in the jet flow plotted against the normalized distance from the nozzle. This figure also includes the results obtained for a jet engine exhaust (Reference 10) and for model rocket and Mach 3 air jet flows (Reference 11) from the near field noise measurements. The higher Strouhal number results are in agreement, but at the lower Strouhal numbers some difference is apparent. The results for the two points nearest the nozzle, and in the initial mixing flow, show the greatest difference. This is surprising, since the results for the jet engine suggested that it was particularly for this part of a jet flow that the normalization would apply. Otherwise the

results obtained here generally agree with the values for the jet engine and the model air jets: the results for the rockets falling in the upper part of the shaded area at lower Strouhal numbers.

The results of Figure 14, in conjunction with the overall source distribution of Figure 12, will allow the acoustic source spectrum to be predicted for all points in the jet flow. The normalized spectrum results indicate that the region of maximum source intensity for any given frequency f occurs at a distance of

$$x = \frac{1.2 V_e a_o}{f a_e}$$

from the nozzle for such jet flows.

In order to examine the importance of any shock turbulence interaction noise, the experiment was repeated with the jet fired into the room at a total plenum pressure of 300 psig compared to the value of 238 psig for perfectly expanded flow. Shadowgraphs of such a condition had indicated that a shock wave pattern is set up. Figure 15 shows the source distribution for this case of the jet fired into the room directly compared to the source distribution for when the jet was operated at normal pressure and the results indicate little significant difference. In fact, the difference is less than that which is observed between the two source distribution curves obtained for the two experiments of the jet fired into the room and out of the room at normal pressure for perfect expanded flow. This result suggests that the shock turbulence interaction noise must be small and not at all significant compared to the other sources of noise generated by the supersonic jet flow.

As was mentioned earlier, the optimum orifice size was used in producing these results. A series of experiments was completed to examine the effect of orifice diameter and Figure 16 shows some typical results. The values shown in Figure 16a, for a jet orifice separation of 21.5 inches, indicates no apparent difference in the

noise generated within the room for a range of orifice diameters from 4 inches to 9 inches, the jet diameter was estimated to be just over 2 inches at the orifice. Figure 16b shows some results for a greater spacing and with a sharp edge orifice as opposed to the square orifice used in most of the experiments. Here again little difference can be seen in the results. Figure 16c shows some results for when the jet was fired out of the room and here it appears that the larger orifice allows more sound to escape out of the room resulting in a lower level. The results for different orifice edge shapes are shown for two examples in Figure 17. No significant difference can be seen between the values for acoustic power determined using either a sharp edge orifice or a square edged orifice as sketched on the Figures. It was concluded that the edge shape had less effect on the measurements that a small change in orifice diameter.

A final series of experiments were completed to examine the effect of varying total pressure on the sound field produced by the flow, to investigate the noise field produced by turbulent shock interaction when the jet was operated at non-ideal expansion conditions. The results are shown in Figure 18. Figure 18a shows the acoustic power spectra for the total sound power generated by the jet when the jet was operated with different plenum pressures. Here the whole jet was contained within the reverberation room and the results show the spectrum level increasing with approximately the same basic shape as the pressure increases, (jet velocity increases). Figure 18b shows the measured values when the first 21 inches of the jet was excluded from the room, and indicates here that the increase in sound for higher plenum pressures is at higher frequencies, the spectrum shape for the lowest pressure showing a very broad spectrum peaking at lower frequencies than the results for the other pressures used. For these tests, it was recognized that shock waves would be formed in the flow at these non-ideally expanded conditions and Figure 19 (from Reference 8) shows shadowgraphs of the jet flow, and indicates the shock patterns formed.

Figure 20 is a plot of the total acoustic power measured for the two examples examined in Figure 18. These values are plotted against a parameter of exit density squared times exit velocity to the 8th power, and show how the results for the total jet noise follows these expected results. The velocity to the 8th power law is that predicted for jets within this velocity range, under 2000 ft per second. The density correction used is that suggested in Reference 12 and has been found most suitable for the collapse of acoustic noise results for jet engines operating within the same velocity range. The results for the second example, when the first 21 inches of the jet was excluded from the room, show the acoustic power generated increasing more rapidly than the basic power law for the total sound generated. These results show how the downstream portion of the flow becomes more important as the jet velocity, and hence the length of the laminar and supersonic cores, increases, especially at the lower plenum plenum pressures (lower jet velocities).

5.0 DISCUSSION OF RESULTS

First the validity of the experimental technique must be examined. On the basis of the absolute nature of the experiment, the only region for criticism must be the assumption that the sound power measured within the reverberation room is due to that part of the jet within the reverberation room alone. Obviously, certain parts of the sound generated in the upstream flow will be carried downstream and refracted out through the flow to be radiated out of the jet at a point further down from that where they were generated. In addition, a certain amount of sound must leak through the orifice, because of the highly directional nature of the sound field radiated, and it was for this reason that the experiment involving varying the orifice size and edge conditions were completed. Any effects would also be indicated by the differences between the acoustic source distribution obtained from the two basic experiments when the jet was fired into the room and out of the room. Examination of Figure 11 indicates that this difference was only small and in fact was generally less than the experimental error that could be expected. An average line was drawn between the two results obtained, and, the acoustic power curve generated was considered to accurately represent the source distribution existing in the jet flow.

The examination of the results for varying orifice size and the low frequency peaks measured in the results for large separation distances, suggested that certain edge tones or hole effects were generated by the jet passing through the orifice. However, the results of Figure 7 indicate that this sound was centered at a frequency of less than 200 Hz whereas the total acoustic power spectrum of the jet noise is centered at 5000 Hz, which is more than a decade higher. Therefore, it was recognized that orifice effects existed, but because of the significant difference between the two peak frequencies of the extra sound and the jet noise, the hole tone noise could be eliminated by smoothing the low frequency curves into the basic sound level measured when the jet was completely contained within the room.

A shadowgraph evaluation of the flow field from this nozzle (Reference 13) showed that Mach waves, lip interaction disturbances, and shock turbulence interactions all apparently radiated a disturbance which could be seen visually on the shadowgraph pictures. However, the acoustic results measured here would suggest that none of these mechanisms was significant to the total sound field produced.

The sound produced by the radiated shocks from the jet flow initial region, observed on the shadowgraphs, would apparently produce sound at frequencies greater than 10,000 Hz. This result is based on measurements of the distance separating the propogating disturbances. The measured acoustic spectra show that very little sound was radiated at these high frequencies. Additionally, the distribution of acoustic power indicates that at all pressures the total sound is dominated by the sound from the sources at about 20 exit diameters downstream. Any sound due to Mach waves or exit lip shock noise would be radiated from the immediate flow downstream of the nozzle, as indicated by the shadowgraphs. The experiment completed here has shown that this is a region of low noise generation. Further, the experiments at various plenum pressures suggest that the noise from the shock turbulence interactions is insignificant compared to the noise due to the turbulent shear. As a result, it was concluded that the turbulent shear flow was the only significant source of sound radiation.

The measured acoustic power generated differs from the predicted result of Ribner (Reference 1) and Lilley (Reference 2) by following an x^1 rather than an x^0 relationship for the sound generated per unit length of the initial mixing region flow. This difference could be explained as the result of the different flow pattern formed, since the jet used in the experiments reported here was supersonic rather than subsonic. However, the probable reason for the difference will be more concerned with the assumptions of both a constant value of maximum normalized turbulent intensity and of similar flow profiles over a range of Mach numbers.

In deriving the x^0 laws, the assumptions of the stress Tensor T proportional to the square of the turbulence intensity u^2 proportional to the velocity squared U^2 are made. The basis of the second assumption is the similarity of the flow in the initial mixing region. However, measured results of turbulence show that the intensity of the turbulence is not a constant through this region, but that the values increase from a minimum at the nozzle to reach a maximum at some distance downstream from the nozzle exit. For a small cold round subsonic jet, the root mean square intensity of the longitudinal velocity fluctuations was measured to be a maximum of 0.08 at the nozzle exit rising to 0.14 compared to the jet exit velocity at a distance of two diameters from the nozzle, (Reference 14). Further downstream, the intensity remained essentially constant to the end of the initial mixing region, and over this part of the flow the results of uniform generation of sound would be expected to apply.

The normalized intensity of the turbulence in the initial mixing region of a supersonic jet will be smaller than for a subsonic jet. This is related directly to the high speed of the jet; the supersonic velocities not allowing disturbances to propogate as effectively as in a subsonic flow. The resultant turbulent mixing action is therefore reduced, the mixing process is slowed and the initial supersonic mixing region and laminar core of the jet lengthened. As the jet mixes and slows, the turbulence strength increases and eventually, at the subsonic core tip, is similar to that for a subsonic jet mixing flow. This increasing turbulent intensity will account for the increasing source strength with downstream distance for a supersonic jet, and additionally cause the major source producing region to occur at a point distant from the nozzle and the initial flow.

This effect is obviously associated with the real nature of jet flows, and will differ for different nozzles and jet speeds. The requirement to measure turbulence properties in the jet flow, and especially in the initial mixing region is therefore indicated. It is proposed to continue these experiments with other jets, both subsonic and supersonic, and to include measurements of the jet turbulence as well as the sound and source field.

6.0 CONCLUSIONS

Two significant points are concluded from these experiments. First, the location of sources in a jet flow has been experimentally demonstrated for the first time, and the results show the major region of acoustic power generation for a high speed supersonic jet (Mach 2.5, 1860 fps) at approximately 20 diameters downstream. Secondly, the experiment shows the potency and flexibility of the reverberant experimental technique for location of sources in free turbulent jet flows.

The results show that the noise of such high speed jets is produced primarily by the region close to the supersonic tip, and that the initial mixing region is a minor source of acoustic power. The flow was carefully chosen to be fully expanded so no shock structure was present, and it was therefore concluded that all acoustic sources, except for those due to the turbulent mixing, were eliminated in the first series of tests. The jet was later run at non-perfect expansion conditions to determine the effects of other sources, such as nozzle shock waves and turbulence-shock wave interactions of under and over-expanded nozzles. No significant differences were observed for the source distribution in these cases and it was therefore concluded that the turbulent mixing process is the major source of noise production for high speed jet flows.

The results presented here are from the initial part of a continuing program and these experiments will be extended to include subsonic and supersonic hot jets. It is anticipated that this program will provide significant results that should help in the understanding of aerodynamic noise generation by jets.

REFERENCES

1. Ribner, H.S., "On the Strength Distribution of Noise Sources Along a Jet," University of Toronto, UTIA Rep. 51, (1958).

2. Lilley, G.M., "On the Noise from Air Jets," British ARC, 20 376, (1958).

3. Lighthill, M.J., "On Sound Generated Aerodynamically - 1, General Theory," Proc. Roy. Soc. A211, (1952).

4. Lighthill, M.J., "On Sound Generated Aerodynamically, - 2, Turbulence as a Source of Sound," Proc. Roy. Soc. A222, (1954).

5. Ffowcs-Williams, J.E., "The Noise from Turbulence Convected at High Speed," Phil. Trans. Roy. Soc. A255, (1963).

6. Mayes, W.H., et al., "Near-Field and Far-Field Noise Surveys of Solid-Fuel Rocket Engines for a Range of Nozzle Exit Pressures," NASA TN D-21, (1959).

7. Morgan, W.V.,and Young, K.J., "Studies of Rocket Noise Simulation with Substitute Gas Jets and the Effect of Vehicle Motion on Jet Noise." Wright Patterson Air Force Base, Report ASD-TDR-62-787, (1963).

8. Ollerhead, J.B., "On the Prediction of the Near Field Noise of Supersonic Jets," NASA CR 857 (1967).

9. Howes, W.L., "Similarity of the Far Noise Fields of Jets," NASA TR R-52 (1960).

10. Eldred, K. Mck., et al., "Suppression of Jet Noise with Emphasis on the Near Field," Wright Patterson Air Force Base, Report ASD-TDR-62-578, (1963).

11. Potter, R.C. and Crocker, M.J., "Acoustic Prediction Methods for Rocket Engines, Including the Effects of Clustered Engines and Deflected Exhaust Flow," NASA CR 566, (1966).

12. SAE, "Jet Noise Prediction," AIR 876 (1965).

13. Lowson, M.V., and Ollerhead, J.A., "Visualization of Noise from Cold Supersonic Jets," to be published in J. Acoust. Soc. Am. (1968).

14. Potter, R.C., "Measurements of the Turbulence in Interfering Mixing Regions of Jets," M.Sc. Thesis, University of Southampton, England (1963).

TABLE I. TEST RUNS

Run No.	Orifice Jet Exit Distance x in. *	Orifice Diameter D in.	Orifice Edge **	Plenum Pressure psig ***
1, 7	Runs not included in analysis, later repeated.			
8	-0	2.5	F	N
9	-4.5	2.5	F	N
10	-9.	3.2	F	N
11	-13.	4.0	F	N
12	-21.5	5.0	F	N
13	-30.	7.0	F	N
14	-39.	9.0	F	N
15	-13.	5.0	F	N
16	-13.	7.0	F	N
17	-13.	9.0	F	N
18	-13.	4.0	F	170
19	-13.	4.0	F	300
20	-60.	9.0	F	N
21	-21.5	9.0	F	N
22	-21.5	7.0	F	N
23	-21.5	4.0	F	N
24	-21.5	5.0	F	N
25	-21.5	5.0	F	100
26	-21.5	5.0	F	170
27	-21.5	5.0	F	300
28	-21.5	5.0	F	400
29	-9.	3.2	S	N

TABLE I. TEST RUNS (Continued)

Run No.	Orifice - Jet Exit Distance x in. *	Orifice Diameter D in.	Orifice Edge **	Plenum Pressure psig ***
30	-21.5	5.0	S	N
31	-39.	9.0	S	N
32	0	2.5	F	N
33	4.5	2.5	F	N
34	9.	3.2	-	N
35	13.	4.0	F	N
36	21.	5.0	F	N
37	30.	7.0	F	N
38	39.	9.0	F	N
39	21.	5.0	F	100
40	21.	5.0	F	170
41	21.	5.0	F	300
42	21.	5.0	F	400
43	0	2.5	F	100
44	0	2.5	F	170
45	0	2.5	F	300
46	0	2.5	F	400
47	9	3.2	S	N
48	21.5	5.0	S	N
49	39	9.0	S	N
50	60	9.0	S	N
51	21.5	4.0	F	N
52	21.5	9.0	F	N
53	21.5	7.0	F	N

TABLE [illegible] TEST RUNS [illegible]

Run No.	[illegible] Exit Distance X [illegible]	[illegible] Diameter D	[illegible] Edge **	[illegible] Power [illegible] ***
54	0	2.5	F	N
55	0	2.5	F	300
56	4.5	2.5	F	N
57	4.5	2.5	F	300
58	9.	3.2	F	N
59	9.	3.2	F	300
60	13.	4.0	F	N
61	13.	4.0	F	300
62	21.	5.0	F	N
63	21.	5.0	F	300
64	30.	7.0	F	N
65	30.	7.0	F	300
66	39.	9.0	F	N
67	39.	9.0	F	300
68	60.	9.0	F	N
69	60.	9.0	F	300
70	21.	4.0	S	N
71	21.	5.0	S	N
72	21.	7.0	S	N
73	21.	9.0	S	N
74	30.	9.0	S	N
75	30.	7.0	S	N
76	30.	5.0	S	N
77	21.	4.0	S	100

TABLE I. TEST RUNS (Continued)

Run No. -	Orifice - Jet Exit Distance x in. *	Orifice Diameter D in.	Orifice Edge **	Plenum Pressure psig ***
78	21.	4.0	S	170
79	21.	4.0	S	N
80	21.	4.0	S	300
81	21.	4.0	S	400
82	50.	9.0	F	300

* Negative x indicates the jet fired from within the room out through the orifice, positive x is for jet directed through the orifice into the room.

** F is flat (square 90 degree) edge to orifice

S is sharp (45 degree) edge to orifice

*** N means plenum pressure adjusted to give perfect expansion, checked by static pressure at nozzle lip, this pressure was approximately 235 psig.

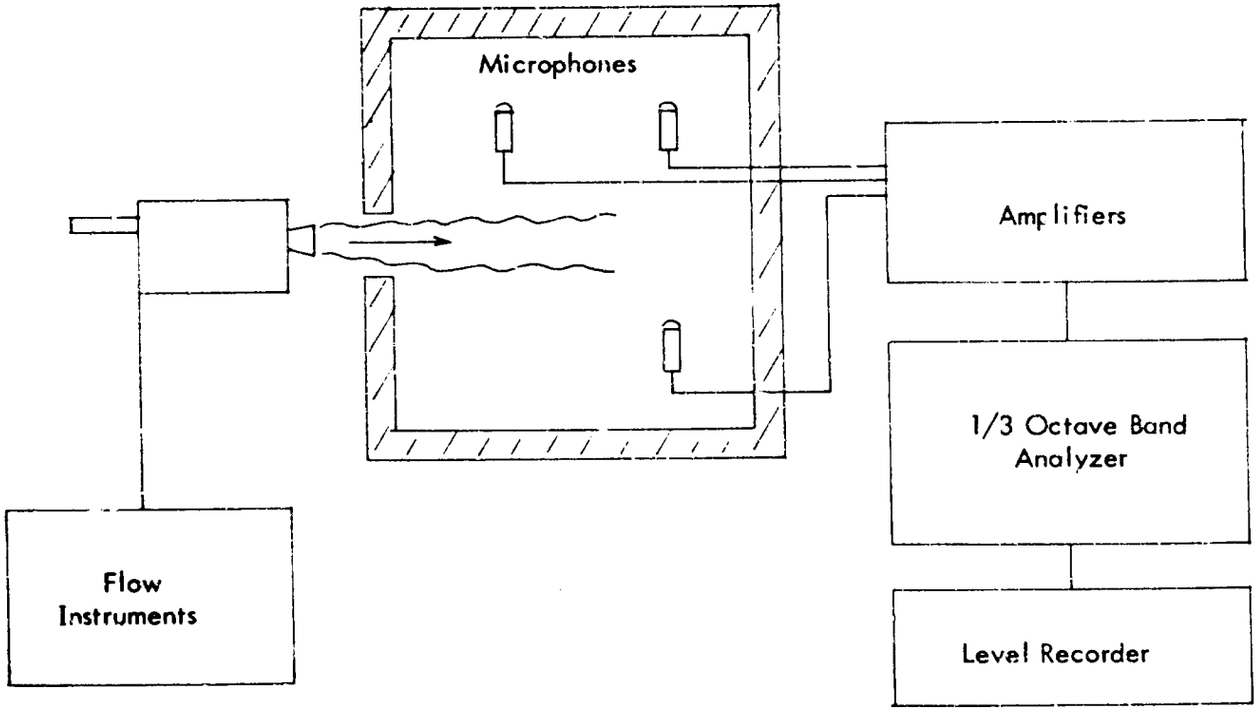

Figure 1, Line Diagram of Setup

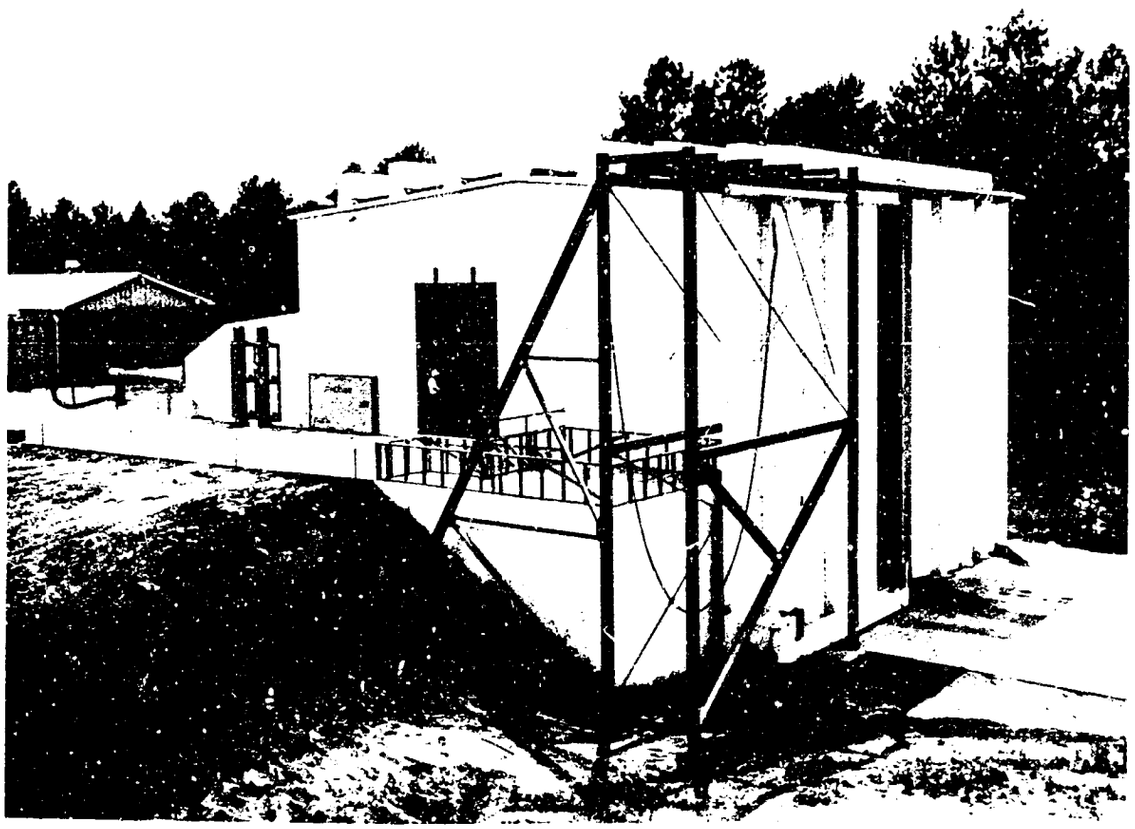

Figure 2. Reverberation Room - External View

Figure 3. Reverberation Room, Internal View

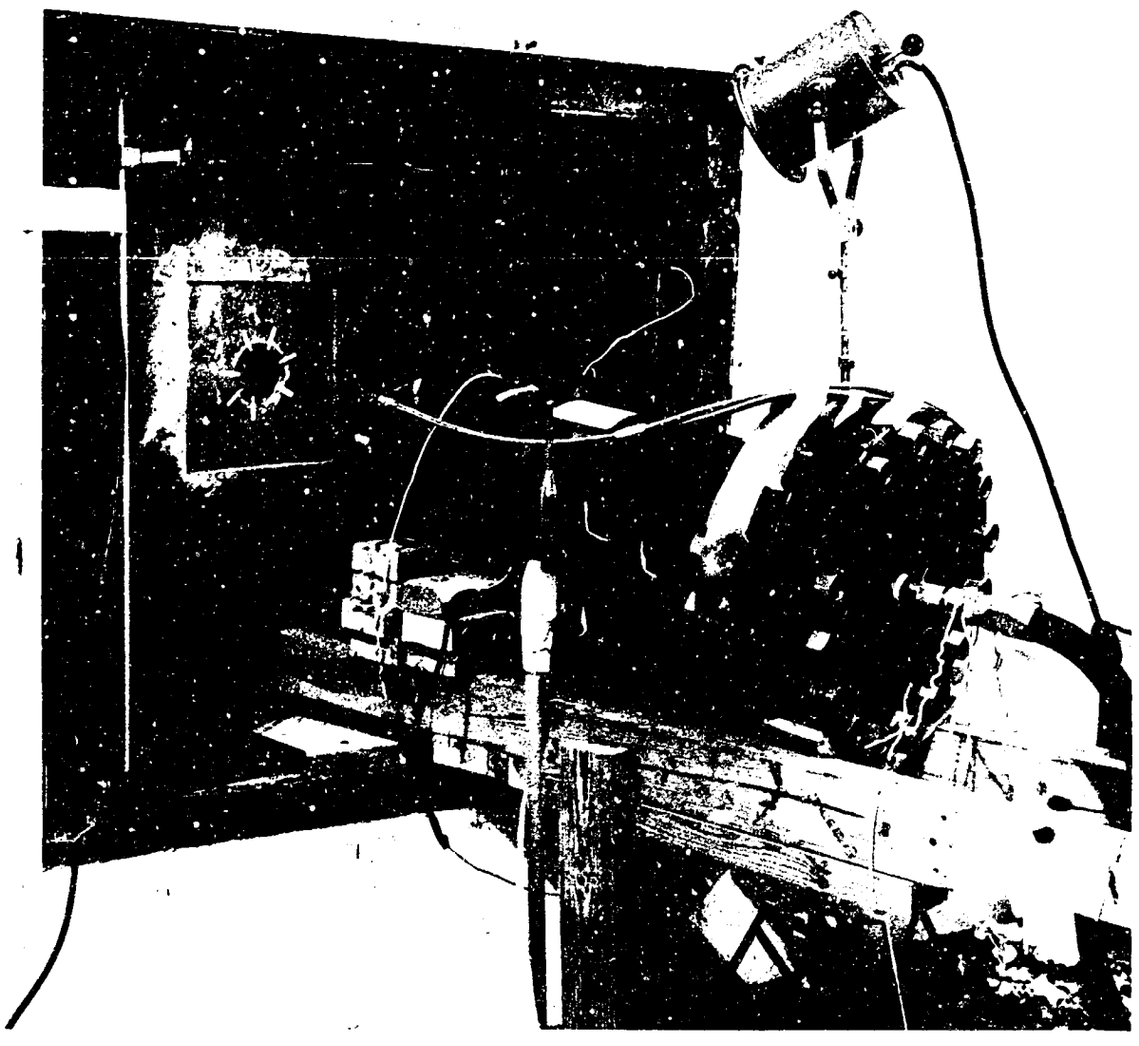

Figure 4. Plenum and Nozzle, Showing the Orifice. The Orifice Plate is Flush with the Inside Wall of the Reverberation Room.

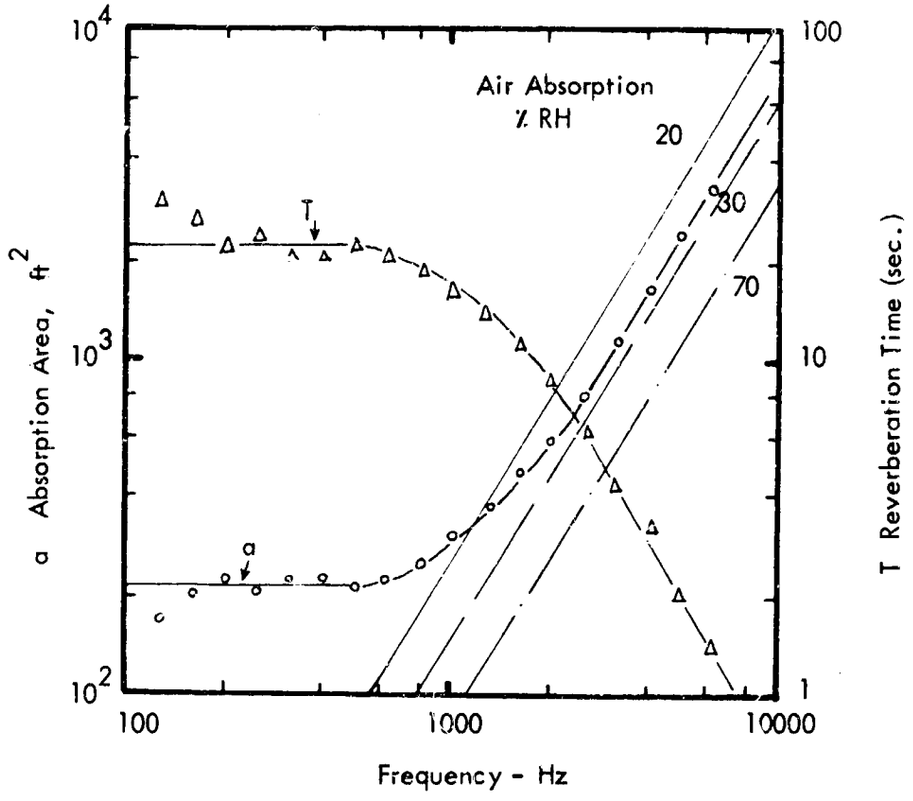

Figure 5, Wyle 100,000 Cubic Ft.
Reverberation Room Characteristics

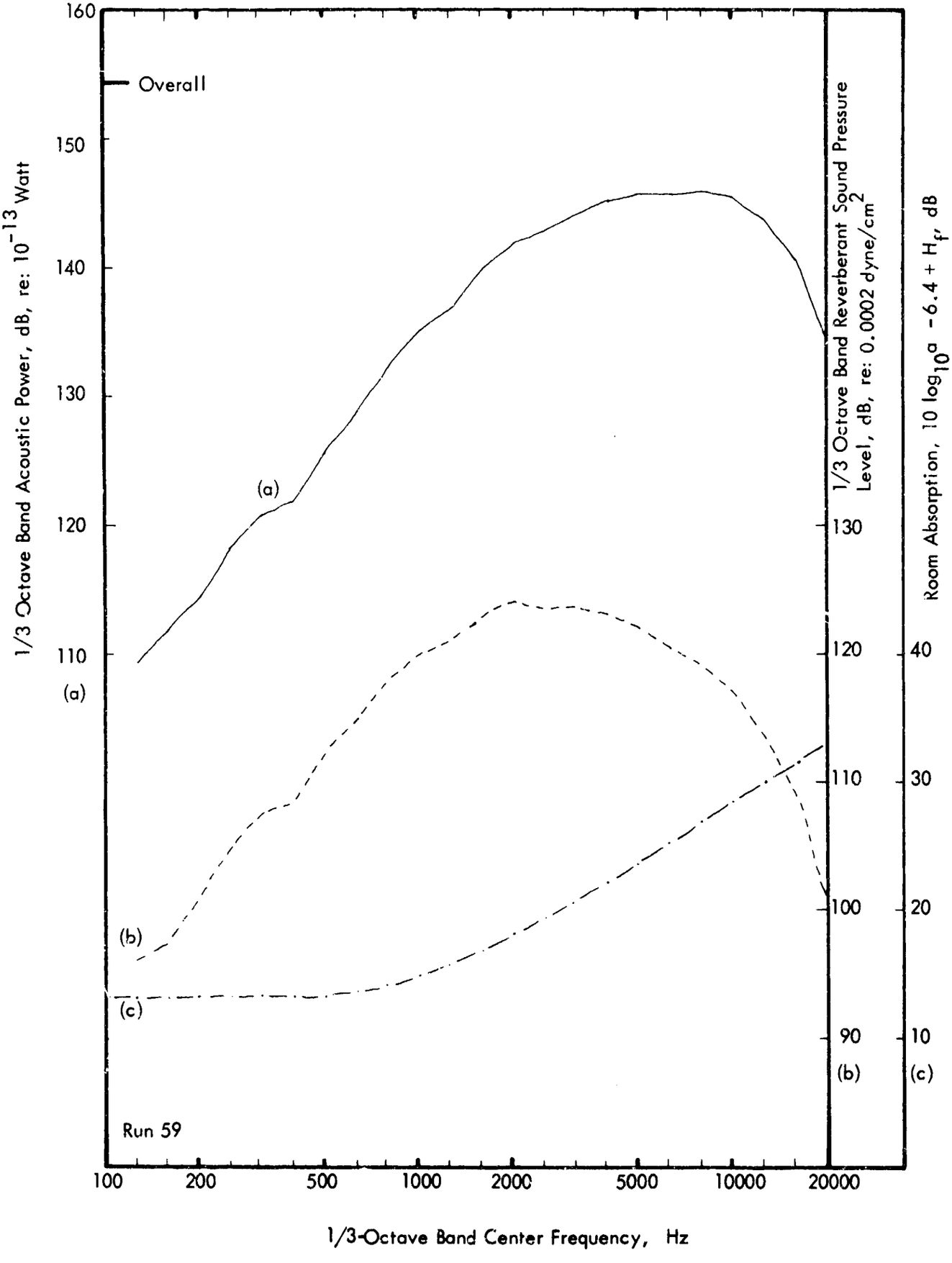

Figure 6, Typical Result

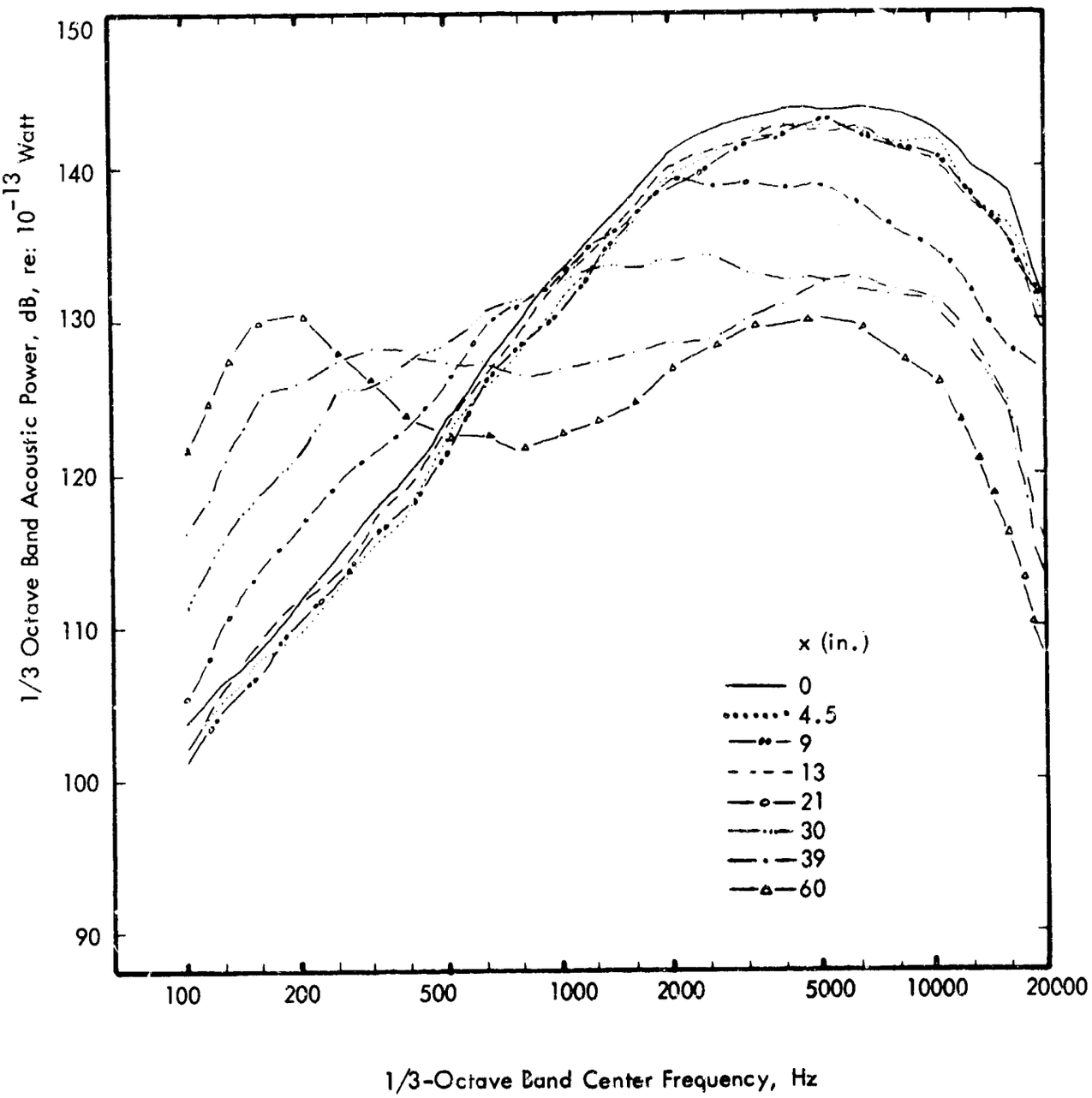

Figure 7, Measured Acoustic Power Spectra - Jet into Reverberation Room

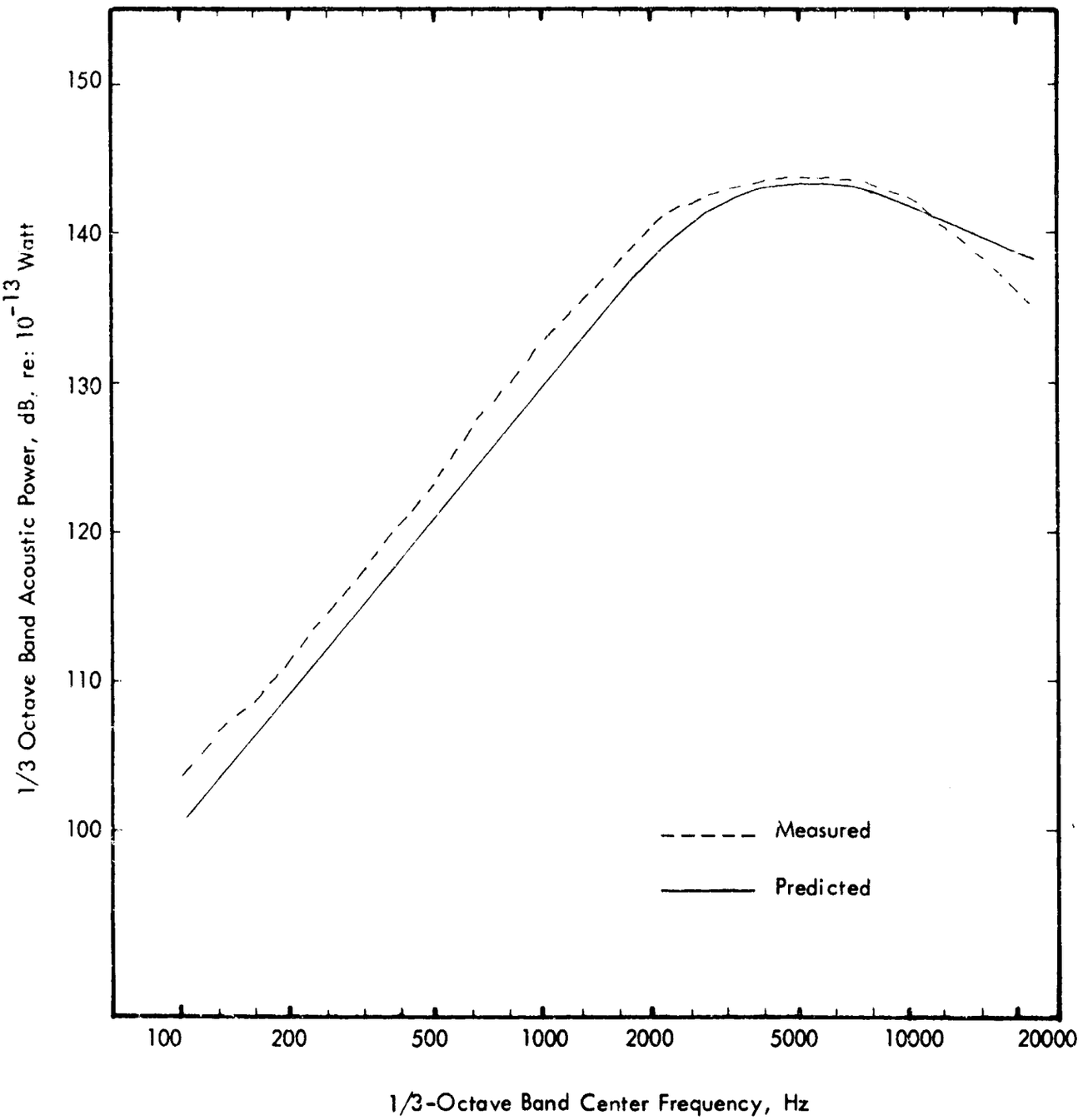

Figure 8, Spectrum of Total Acoustic Power of the Jet at Normal Operation

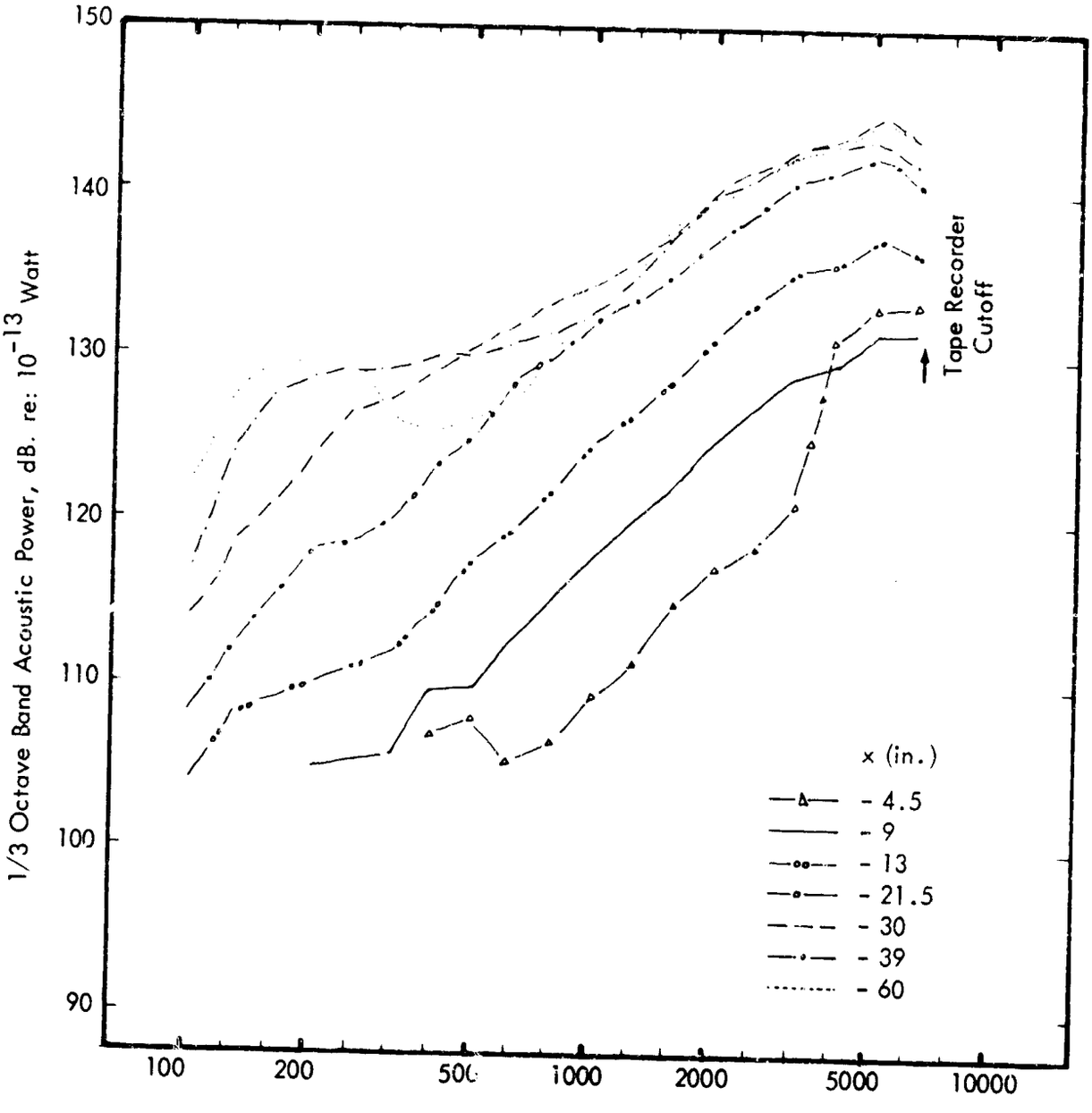

Figure 9, Measured Acoustic Power Spectra - Jet Out Of Reverberation Room

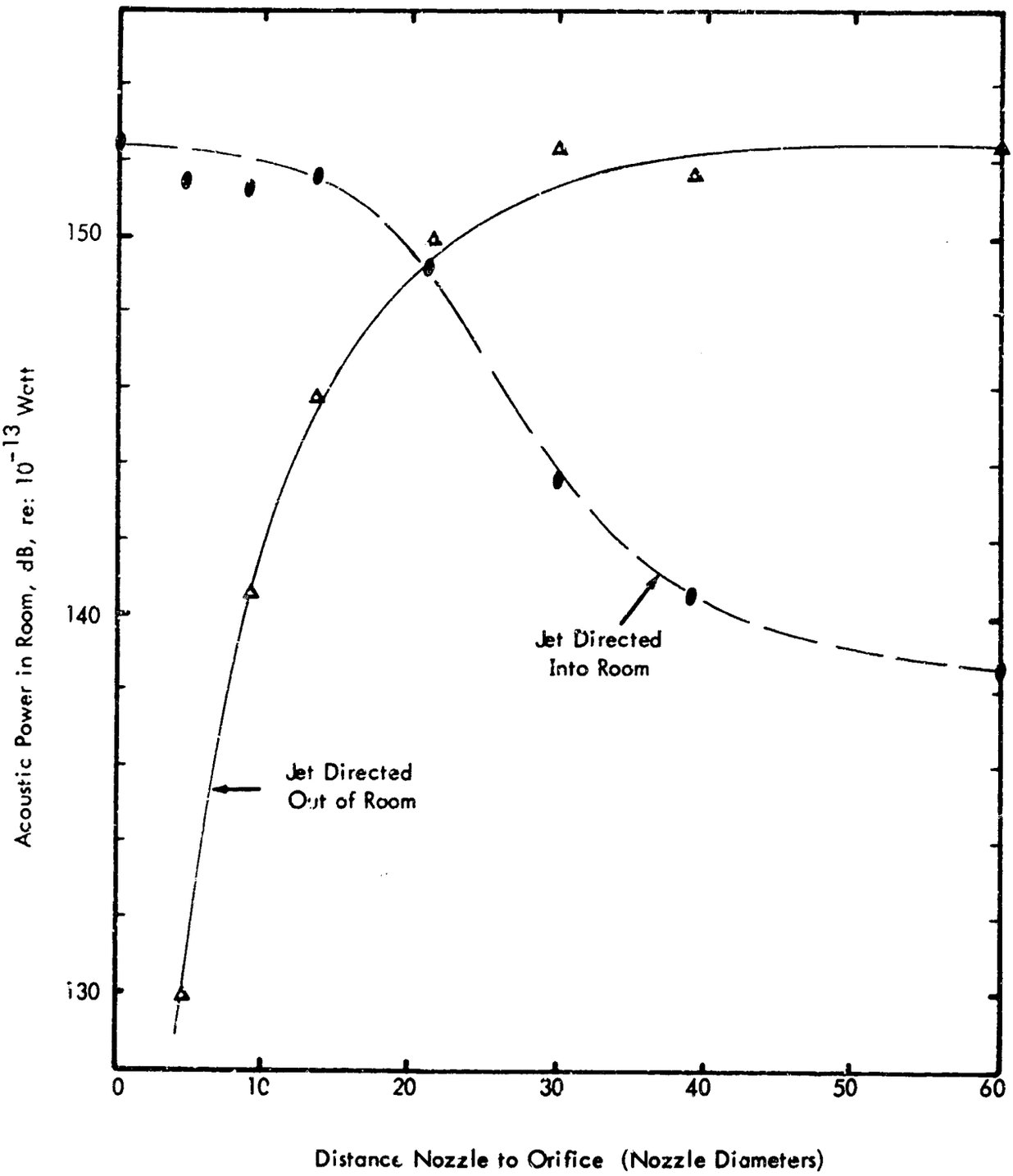

Figure 10, Overall Power Levels Measured

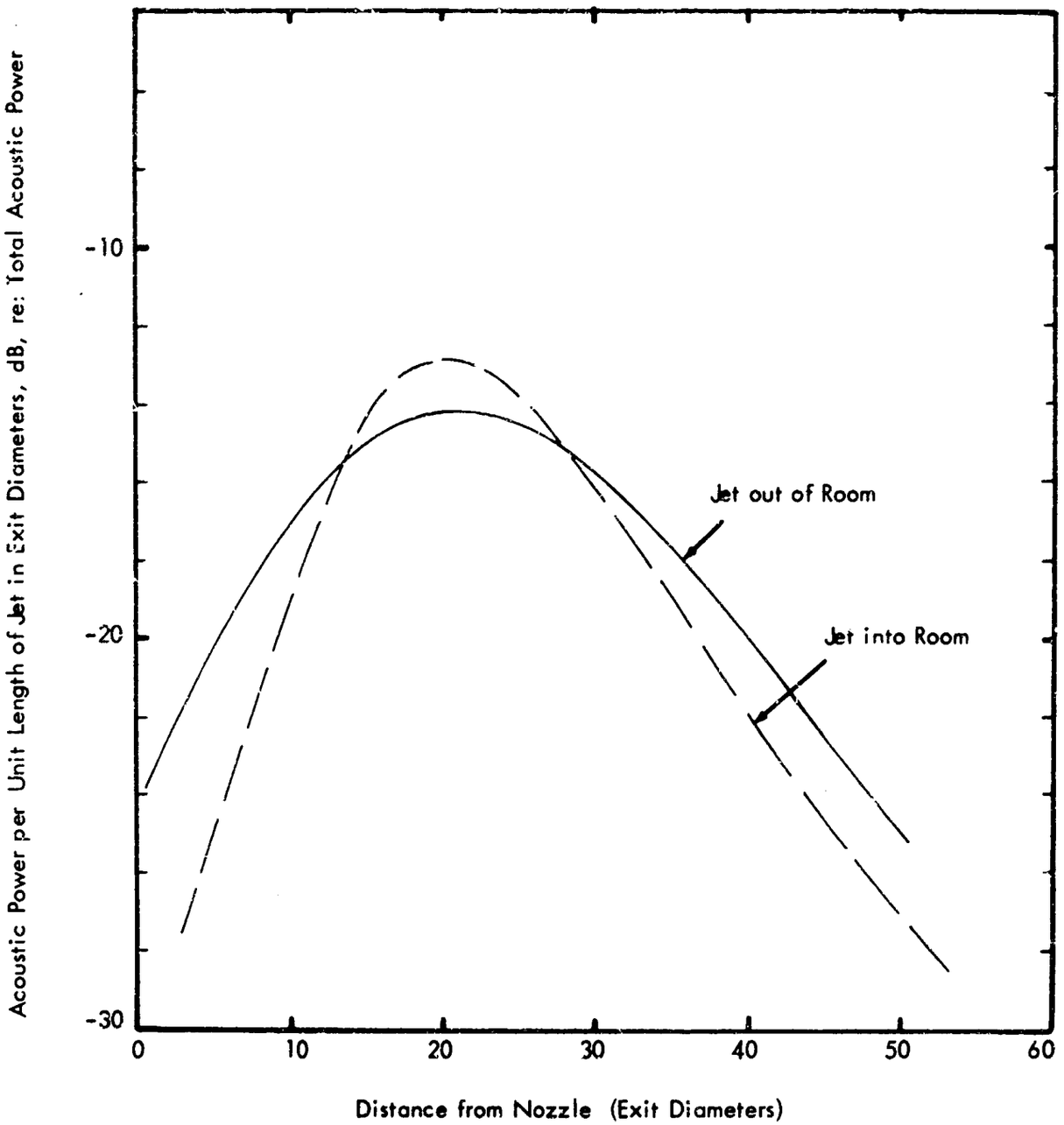

Figure 11, Acoustic Power per Unit Length of the Jet

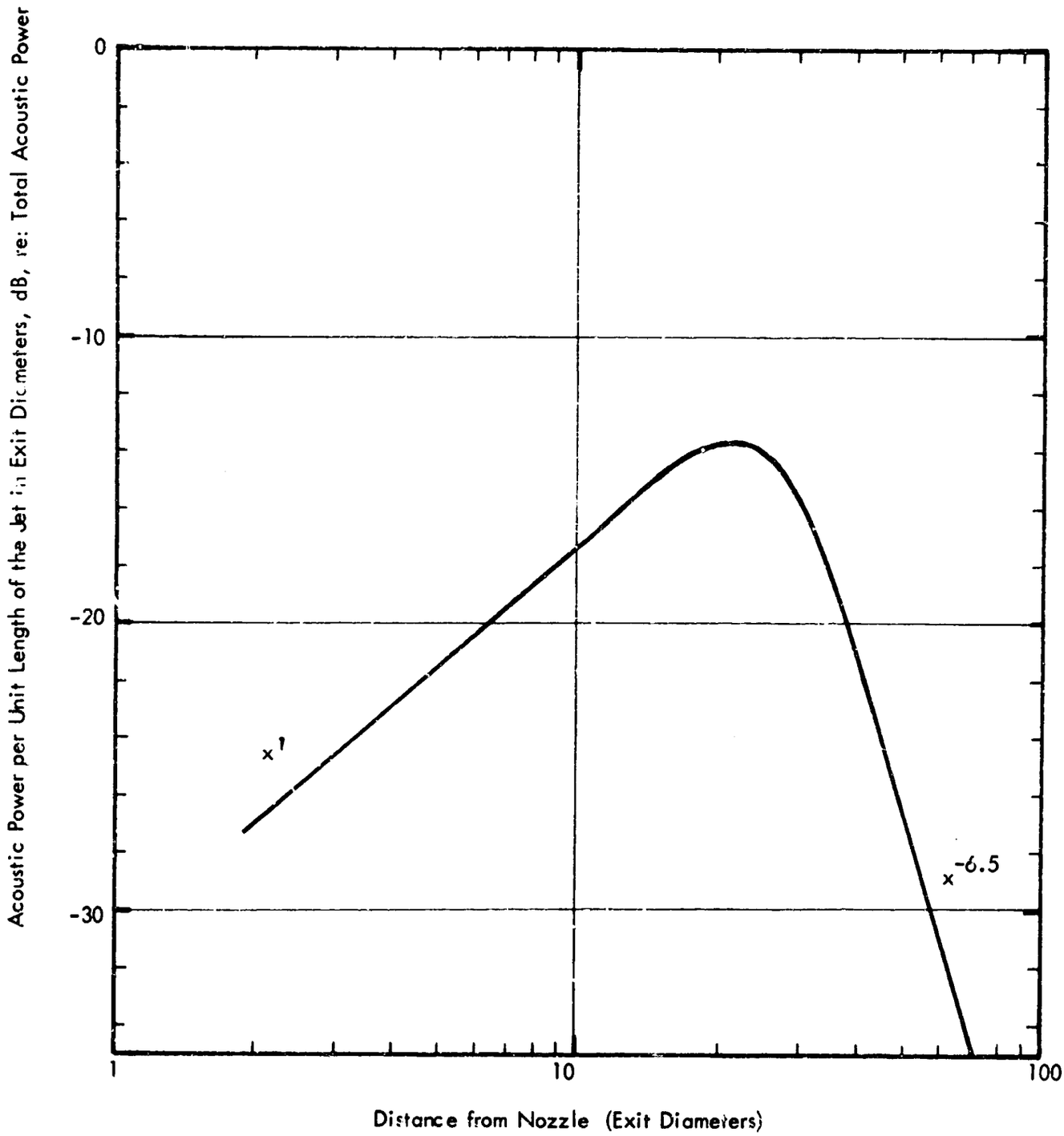

Figure 12, Acoustic Power per Unit Length of the Jet

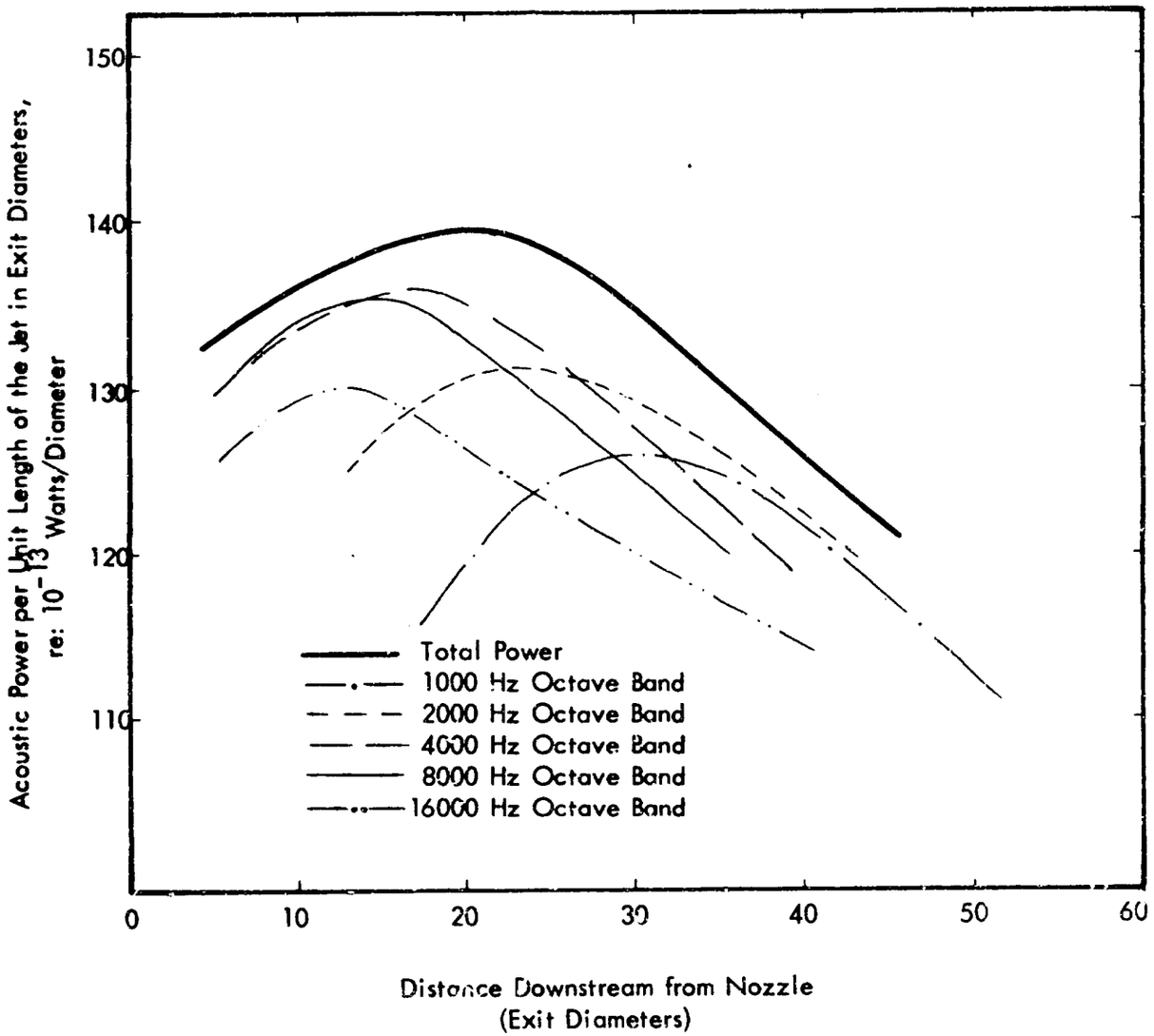

Figure 13, Octave Band Analysis Power Generated per Unit Length of the Jet

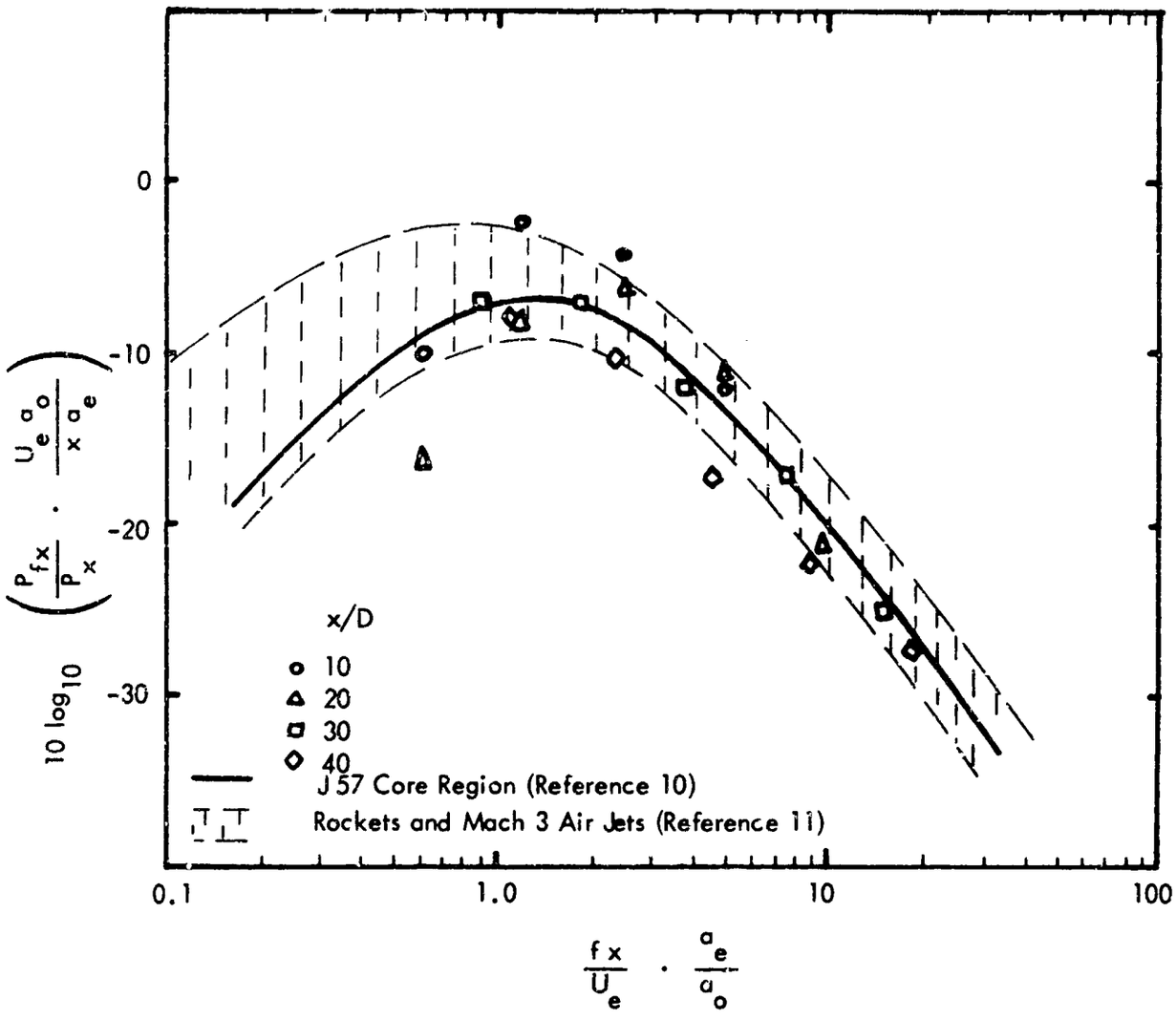

Figure 14, Normalized Acoustic Source Spectrum

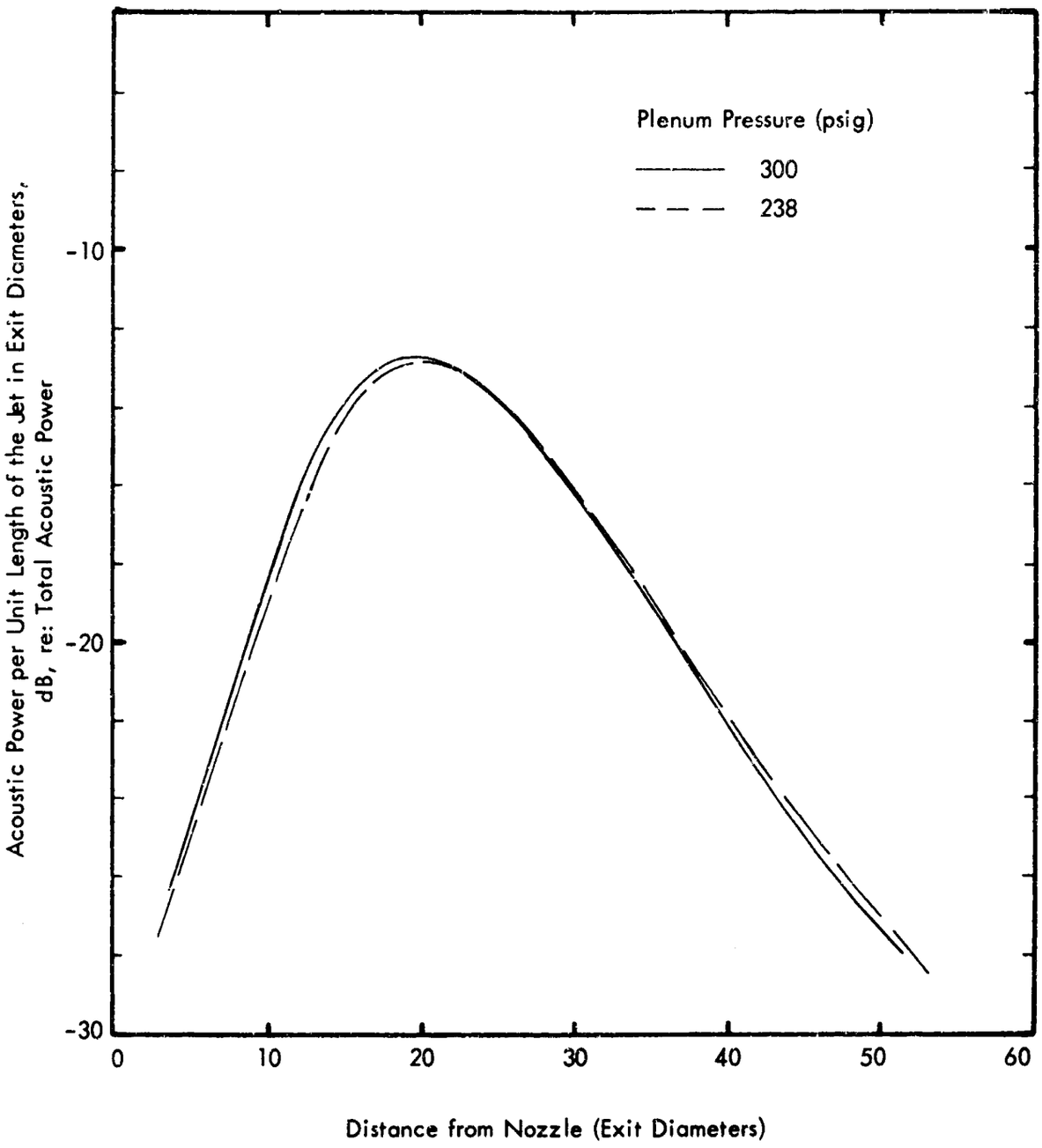

Figure 15, Source Distribution at Two Plenum Pressures

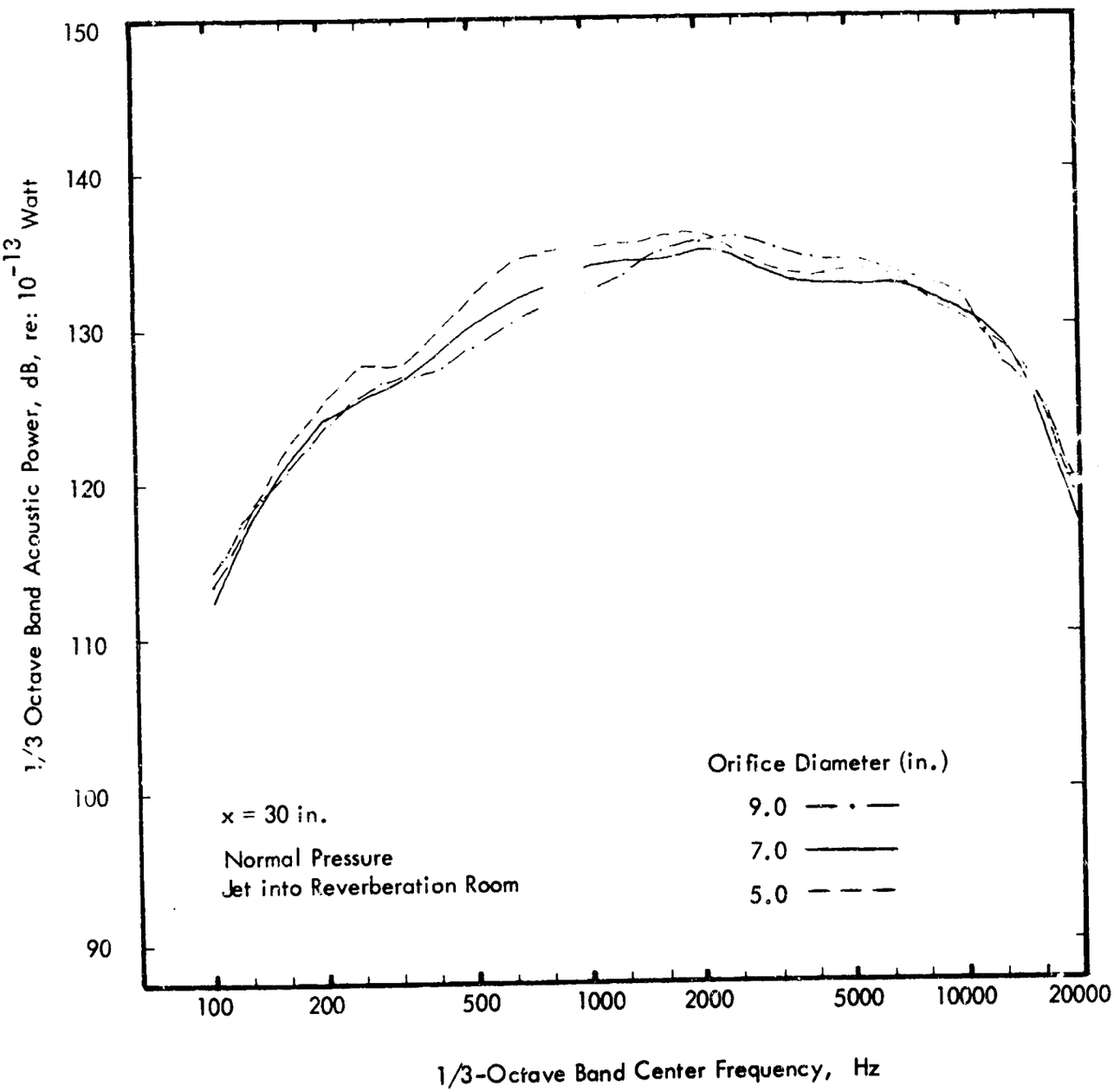

Figure 16 a, Effect of Orifice Diameter, Sharp Edged Orifice

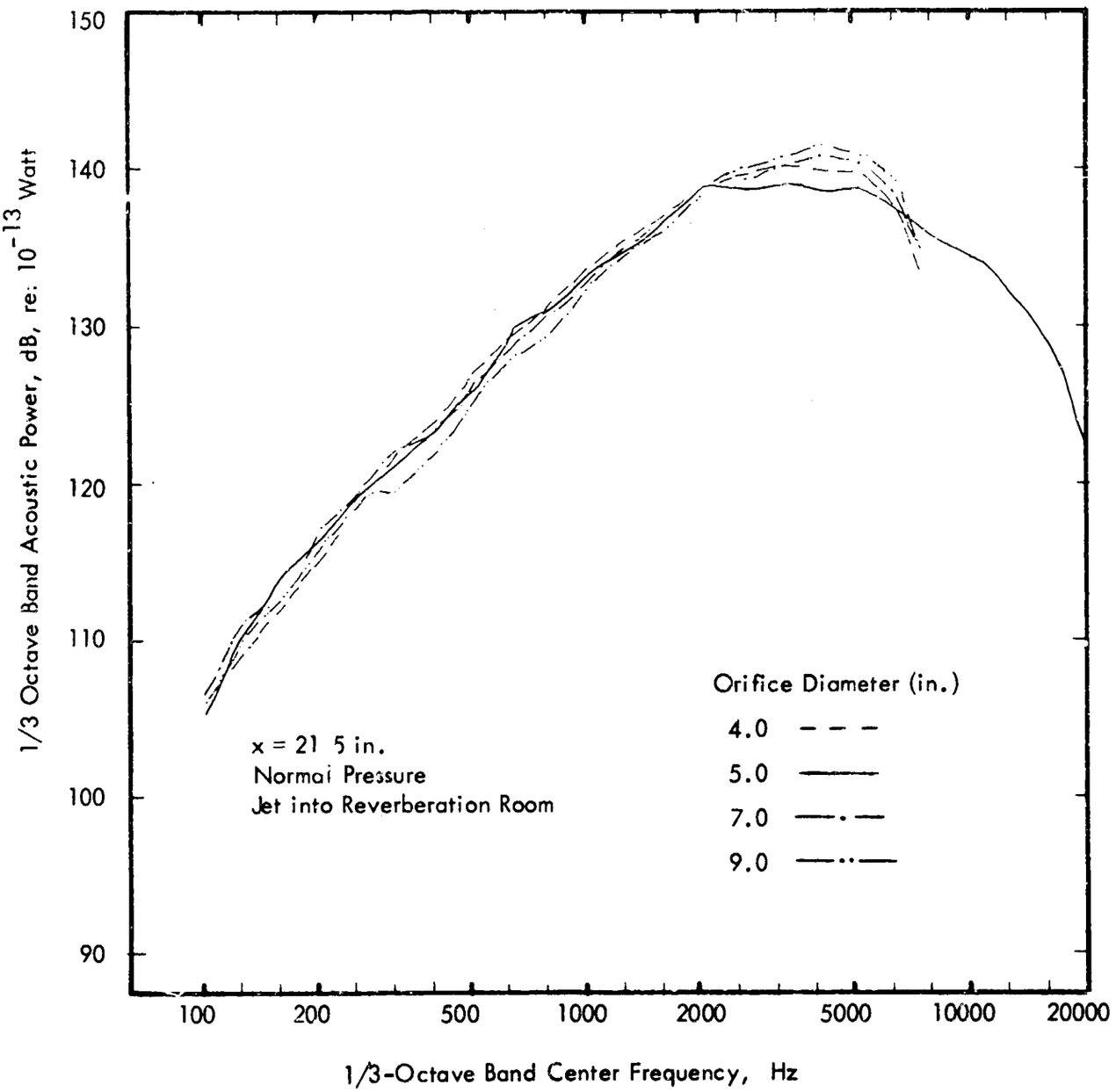

Figure 16 b, Effect of Orifice Diameter, Square Edged Orifice

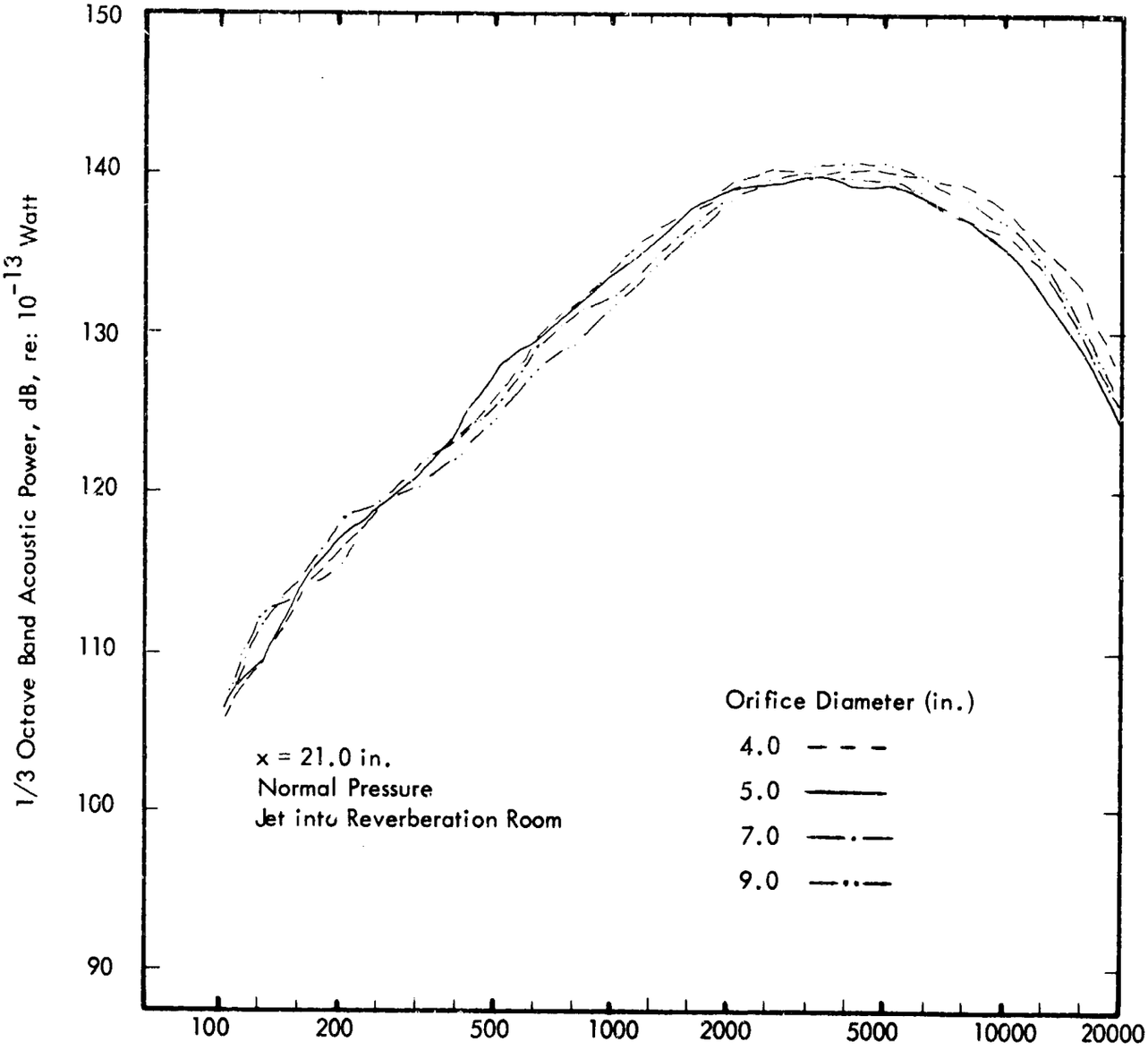

Figure 16 c, Effect of Orifice Diameter, Sharp Edged Orifice

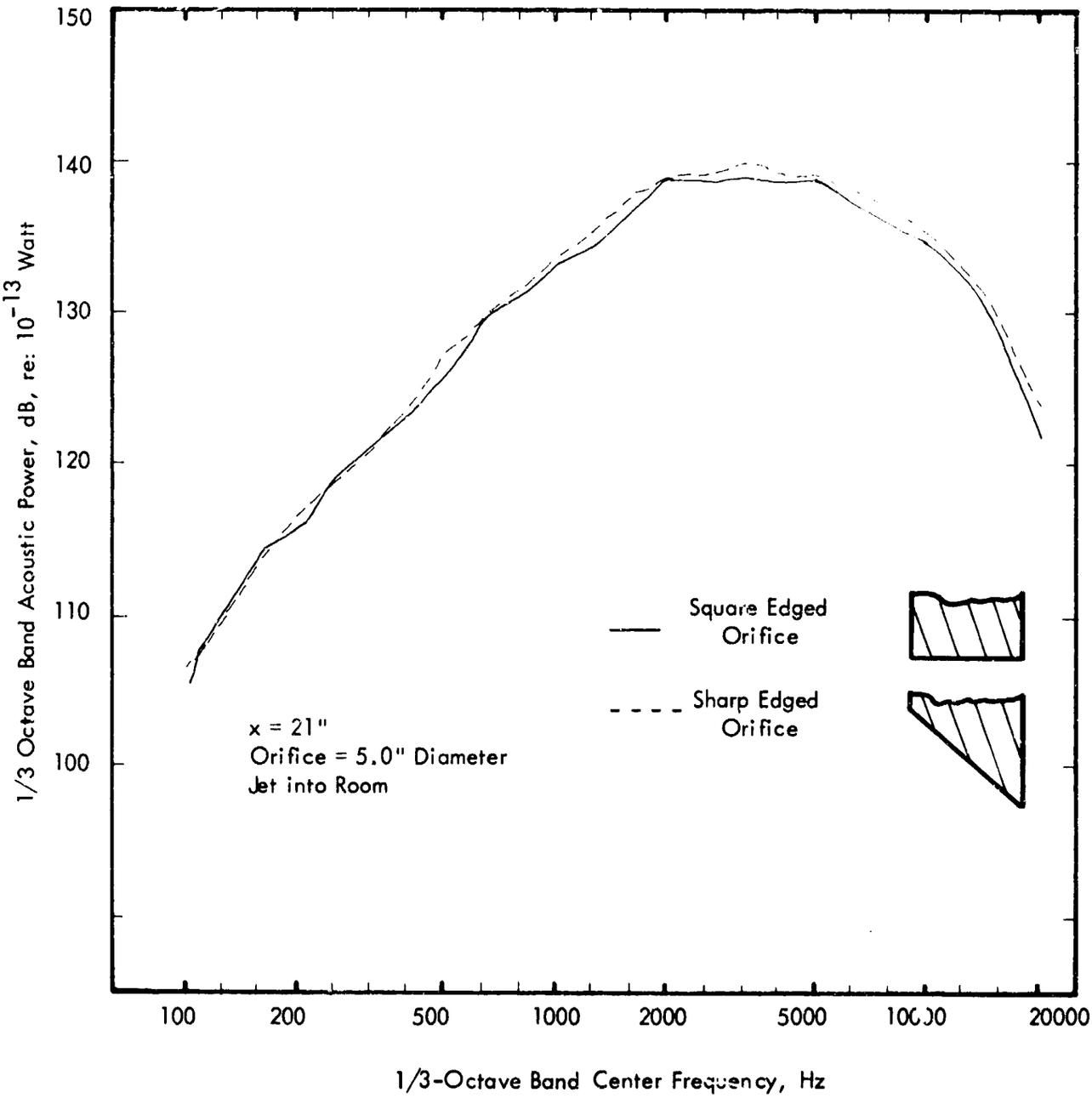

Figure 17 a, Effect of Orifice Edge

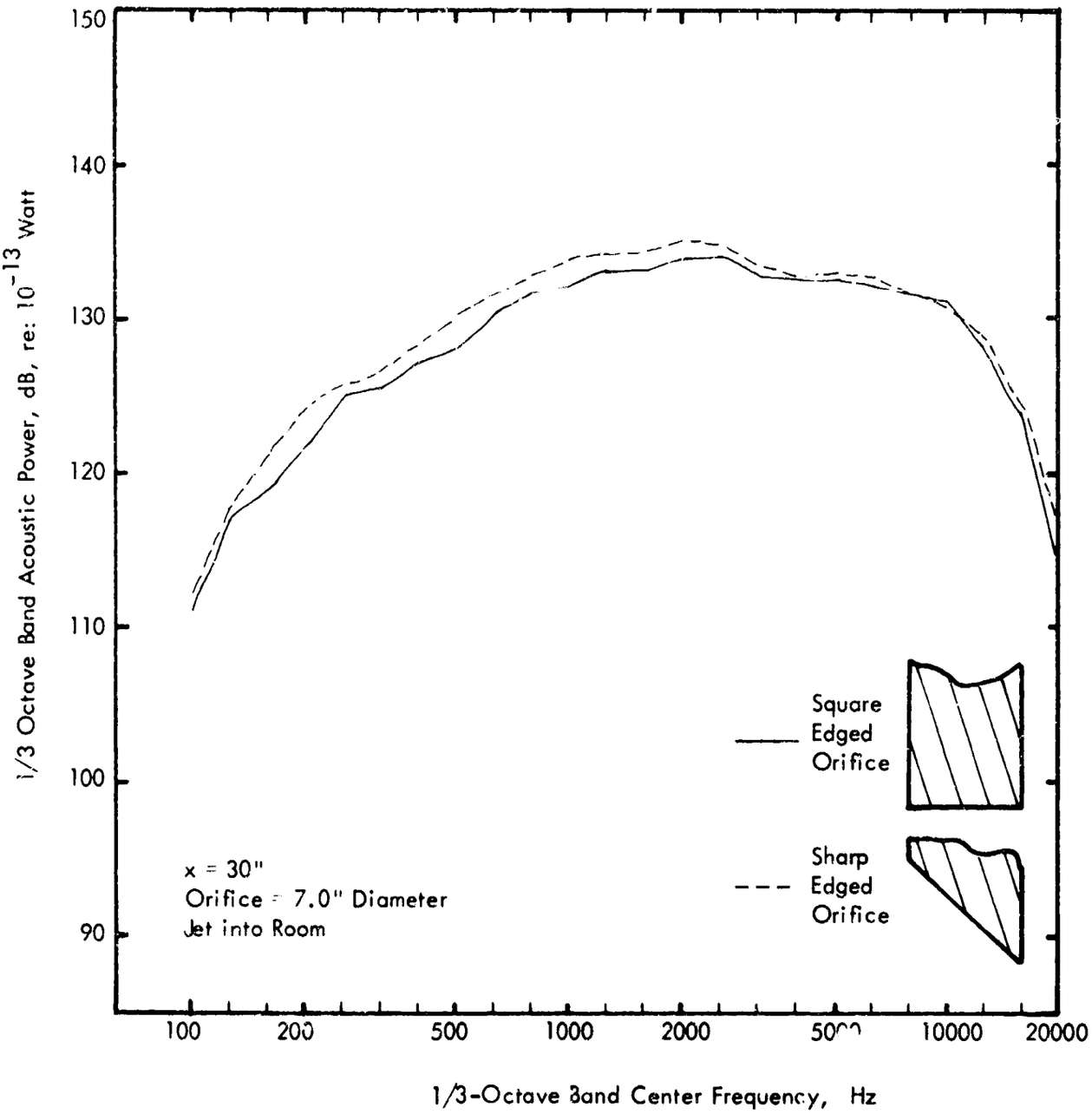

Figure 17 b, Effect of Orifice Edge

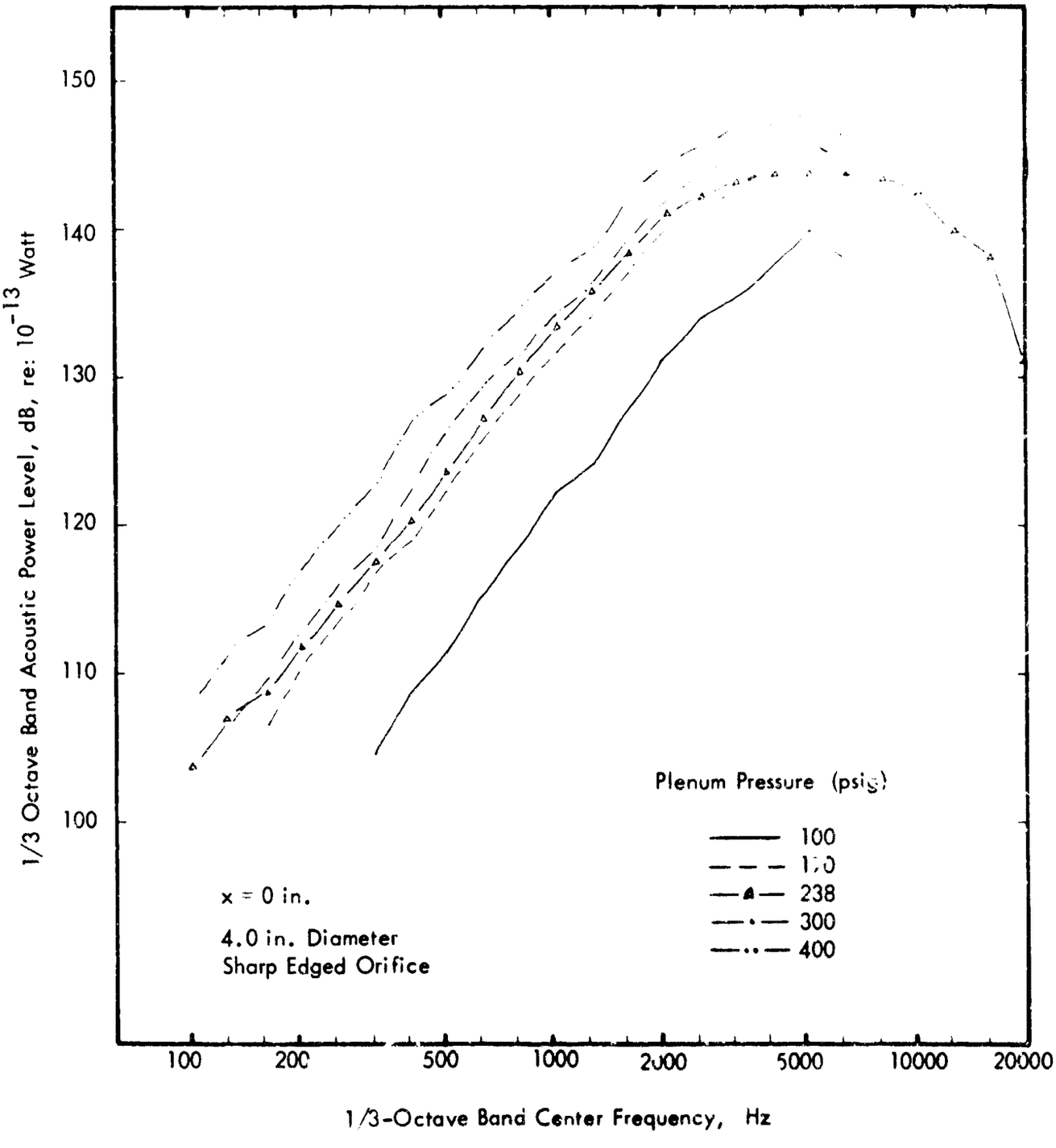

Figure 18 a, Effect of Plenum Pressure Change

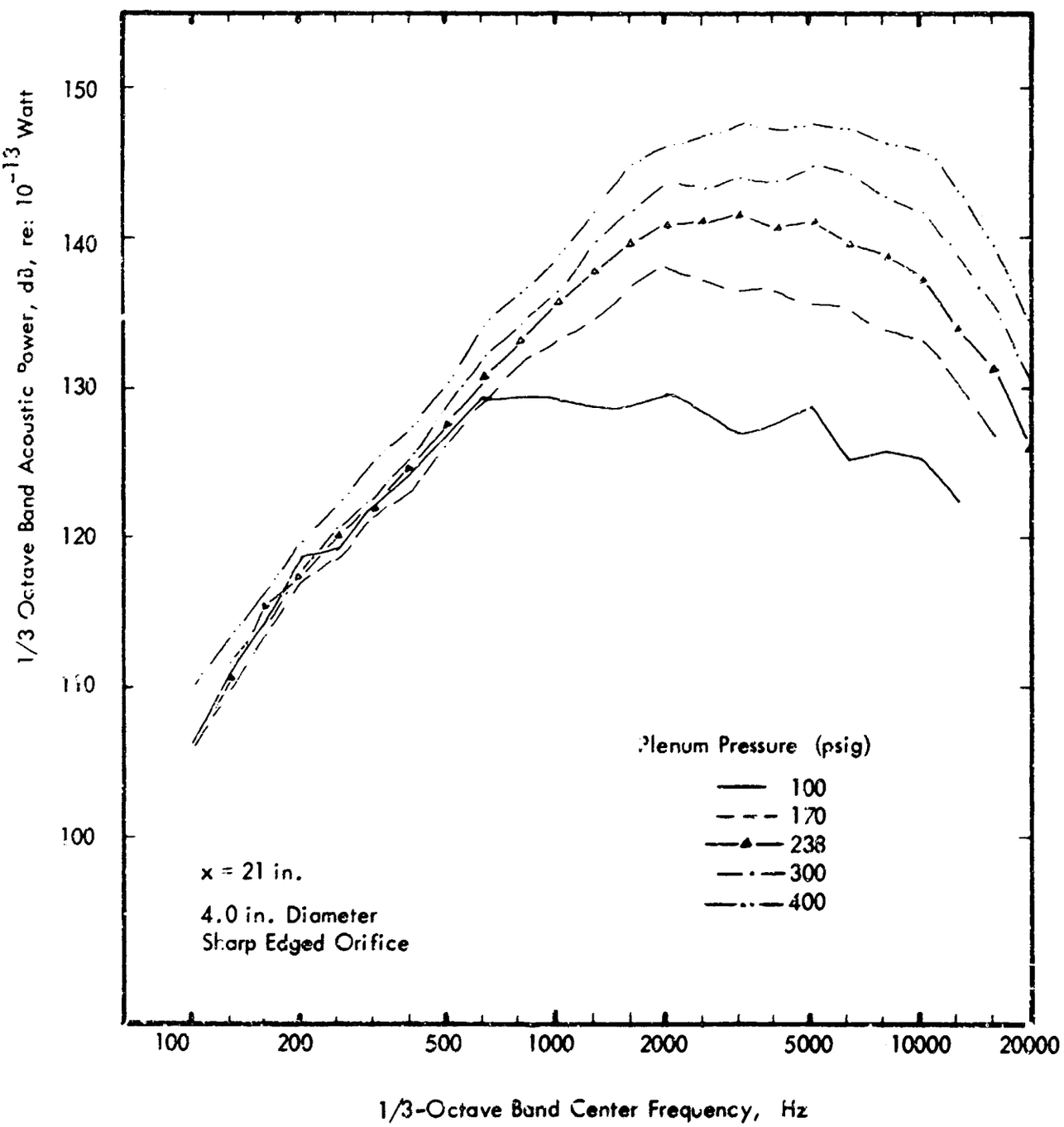

Figure 18 b, Effect of Plenum Pressure Change

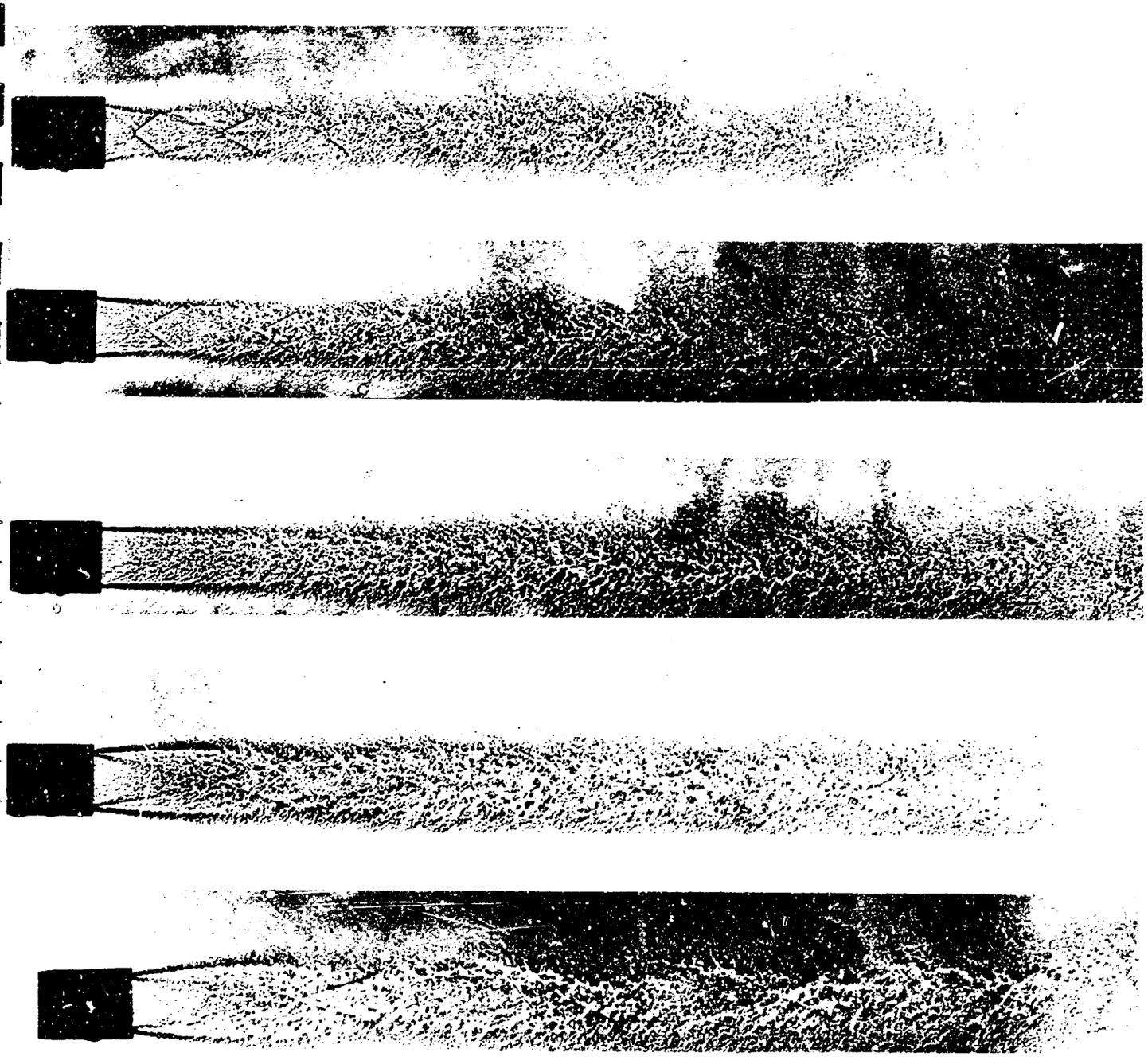

Figure 19. Development of Shock Patterns with Nozzle Exit Pressure. Design Mach Number 2.47, From Top to Bottom; p_E/p_o = 0.497, 0.747, 1.00, 1.53, 1.98 (from Reference 3).

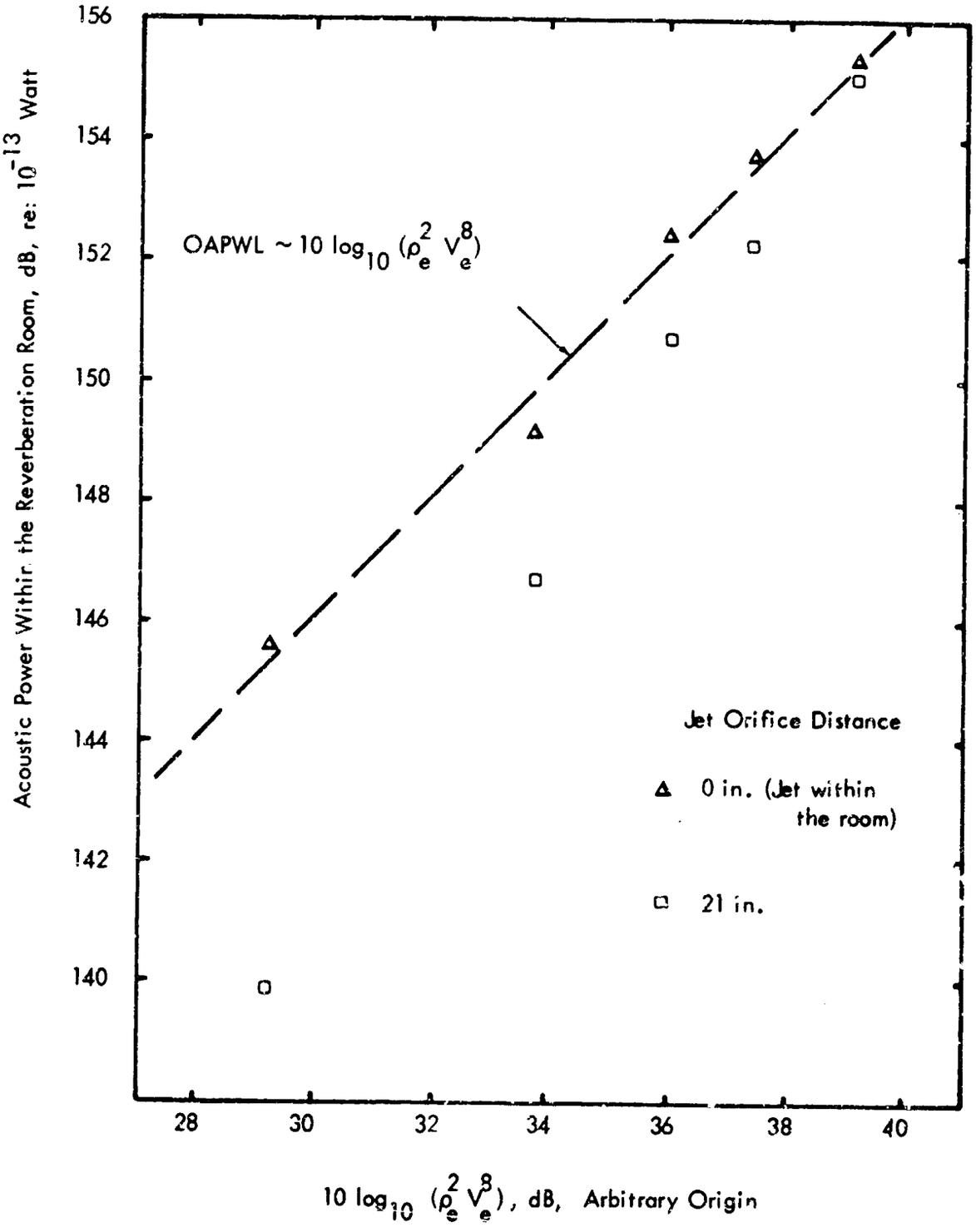

Figure 20, Acoustic Power When Jet Operated at Various Plenum Pressures (Jet Velocities)